Hydraulic Characteristics of Circular Culvert Inlets Relating to Fish Passage

By

Martin J. Hunt

A thesis submitted to the Faculty of Graduate Studies of
The University of Manitoba
in partial fulfilment of the requirements for the degree of

Master of Science

Department of Civil Engineering
Faculty of Engineering
University of Manitoba
Winnipeg, Manitoba

Abstract

This thesis presents the findings of a physical modeling study examining the hydraulic characteristics within the inlet region of a corrugated steel pipe (CSP) culvert with common inlet treatments. Also examined are the effects of embedding the culvert below the stream bed and backfilling the culvert with granular material.

Velocity and turbulence distributions were examined in an effort to better understand how these inlet treatments may affect fish passage. The velocity field of each inlet configuration was dominated by a central jet of high velocity surrounded by low velocity boundary areas. Based on percent area analysis the various projecting end inlet configurations presented the largest area with streamwise velocities less than U_{avg}. The usefulness of the low velocity boundary areas may be limited by significant vertical and spanwise velocities and associated elevated turbulence levels.

Acknowledgments

This study was made possible through the assistance of numerous individuals and organizations.

I would like to thank my supervisor, Dr. Shawn Clark, for his support throughout my years of study and for guiding me into what is becoming a fulfilling career. I would also like to thank my colleges and friends from the Hydraulic Research and Testing Facility, particularly; Garrett Ward, Nicholas Kehler, Carly Delavau, Phil Slota, Jarrod Malenchak, and Scott Toews.

Funding for this study was provided by Manitoba Infrastructure and Transportation, the Federal Department of Fisheries and Oceans, and the National Science and Engineering Council. The CSP culvert used for the model was generously donated by the Corrugated Steel Pipe Institute.

Dedication

This thesis is dedicated to my family. To my parents and grandparents, who have supported me throughout my life and academic career. The roots that you sowed have made it possible for me to pursue my dreams, for that I will be forever grateful. To my brother Stephen, for showing me that the world is vast and worth exploring. And to my wife Megan, for inspiring me to be my best.

Contents

List of Tables

List of Figures

List of Symbols

Symbol	Unit	Description
ΔH	[m]	total head loss related to the inlet
A	[m^2]	cross sectional area
a_{fw}	[m/s^2]	acceleration of a fish relative to the surrounding water
b	[-]	profile drag coefficient
d	[m]	diameter of culvert
d_{50}	[cm]	grain size diameter with 50% non exceedence probability
EDF	[$m\text{-}N/m^3/s$]	energy dissipation factor
F	[-]	Froude number
F_d	[N]	profile drag on a fish
F_g	[N]	force of gravity
F_m	[-]	model Froude number
F_p	[-]	prototype Froude number
F_{vm}	[N]	virtual mass force required to maintain forward motion within an accelerating medium
g	[m/s^2]	acceleration due to gravity
□	[N/m^3]	specific weight of water
k	[m^2/s^2]	turbulent kinetic energy
K	[-]	profile drag constant

k_e	[-]	entrance loss coefficient
L	[m]	total length of a fish
l_r	[m]	characteristic length
Q	[m^3/s]	flow rate
Re^*	[-]	Reynolds number
S	[-]	slope
U_{avg}	[m/s]	average cross sectional streamwise velocity positive in the downstream direction
u	[m/s]	instantaneous streamwise velocity
U_i	[m/s]	average point velocity
$u_i^{'}$	[m/s]	root mean squared of instantaneous velocity
v	[m/s]	instantaneous vertical velocity
v_{fw}	[m/s]	velocity of a fish relative to surrounding water
w	[m/s]	instantaneous spanwise velocity
W	[kg]	weight of a fish
x	[-]	streamwise direction positive in the mean direction of flow
y	[-]	y or vertical direction positive up
z	[-]	spanwise direction horizontally perpendicular to the flow with the positive direction defined to the left when looking in the positive x-direction
ν	[m^2/s^2]	kinematic viscosity of water
ρ	[kg/m^3]	mass density of water

Chapter 1

Introduction

1.1 Background

Stream crossings represent a significant portion of the cost of transportation networks. Corrugated steel pipe (CSP) culverts provide a relatively low cost, hydraulically efficient crossing option. As such, they are commonly selected for small to medium size stream crossings. Traditionally, the goal of culvert crossing design has been to pass some required discharge using the most economical design available. As a result of this design philosophy a large majority of past culvert research has focused on issues relating to their hydraulic performance and optimization.

Recently, concerns regarding the ecological impact of culvert crossings has lead to changes in design philosophy. The *Manitoba Stream Crossing Guidelines for the Protection of Fish and Fish Habitat* (Canadian Department of Fisheries and Oceans and Manitoba Natural Resources, 1996) outlines how fish are affected by the introduction of structures such as culverts into the natural environment. One of the primary ecological concerns attributed to culvert crossings is the potential barrier presented to upstream fish migration resulting from the constriction of the channel. Certain species of fish rely on upstream migration as a means of accessing food, spawning grounds and overwintering habitat. Delays and obstruction of upstream migration can result in reduced spawning success as well as increased predatory vulnerability. The traditional installation of CSP culverts also result in a direct loss of fish habitat as the natural riverbed is replaced by the culvert and road embankments. The improper installation and or maintenance of culverts may result in erosion at culvert outlets. This erosion may in turn result in a perched outlet and conditions exceeding the ability of certain species of fish.

In an effort to minimize the impact of culvert crossings on stream ecology, several jurisdictions have developed regulations to ensure that their design will allow for the upstream passage of migratory fish. In Canada, these regulations set several requirements relating to culvert design. Dependant on jurisdiction requirements can include restrictions on average water velocity, minimum flow depths, minimum embedment depth, and require culverts to be backfilled with a minimum depth of suitable bed material. These regulations are often the controlling factor in culvert design, requiring culvert sizes significantly larger and more expensive than would otherwise be selected.

The increased cost associated with these regulations has served as the motivation for numerous recent studies aimed at developing a better understanding of the hydraulics of culverts as they relate to fish passage. These studies have contributed significantly to the understanding of conditions in the approach and fully developed regions of pipe culverts. Conditions within the inlet region of CSP culverts and how they relate to fish passage regulations have yet to be examined in detail. The limited understanding of the complex conditions within the inlet region of culverts represents a gap in current fish passage research. A detailed examination of the conditions faced by fish traversing a culvert inlet will contribute to ensuring a balance between economical and environmentally sustainable design of circular CSP culvert crossings.

1.2 Objective

The objective of this research project is to examine in detail the hydraulic characteristics of circular CSP culvert inlets as they relate to fish passage. Towards this end, a model study was conducted to examine the flow field within inlet region of a circular CSP culvert model with various inlet configurations under a range of conditions.

The objectives of the research are:

- record detailed measurements of three dimensional water velocities within the inlet region of a model culvert with vertical headwall, 45° wingwall and projecting end inlet treatments,
- examine the structure of the three dimensional velocity and turbulence fields of the various inlet treatments,
- examine the effect of embedment and backfill on the flow field of CSP culvert inlets, and

- provide data to be used for the development and calibration of future numerical modeling studies.

1.3 Overview

Chapter 1 of this text describes the background and motivation for the research. Chapter 2 presents a review of theory and current research related to fish passage and culvert design. Section 2.1 will present background information regarding the hydraulics and design of CSP culvert crossings including traditional design goals, culvert control/flow types, culvert inlet hydraulics, and entrance losses. An overview of the principles of fish passage including principles of fish swimming, the effect of culvert hydraulics on fish passage and the effect of turbulence on fish will be presented in section 2.2. Section 2.3 will examine the methods and findings of other recent model studies relating to culvert fish passage issues. Chapter 3 describes the laboratory setup including model design and apparatus used for the research project. Chapter 4 describes the testing procedure adopted for the project as well as data analysis methods used to process recorded data. Chapter 5 presents the results and analysis of the model study including water surface profiles, entrance losses, velocity fields and turbulence fields. Chapter 6 presents a summary of the study findings, conclusions, and recommendations for future work.

Chapter 2

Literature Review

2.1 Culvert Design and Hydraulics

2.1.1 Background

The analysis of culvert hydraulics has been described by numerous authors (Federal Highway Administration, 2001; Sturm, 2001) as extremely complex. This complexity is a result of the wide range of flow conditions a culvert must accommodate. At any given time, a culvert crossing may contain any combination of the following flow types; gradually varied, rapidly varied, time dependent, open channel, pressurised, super-critical and sub-critical flows.

Culvert hydraulics are further complicated due to the fact that depending on the discharge, physical characteristics, and surrounding environment, the capacity of a culvert may be governed by inlet or outlet control. When operating under inlet control the head-discharge relationship of a culvert is influenced by the inlet shape, inlet edge configuration, and inlet area. A culvert operating under inlet control will act as an orifice when the inlet is submerged and as a weir if the inlet is un-submerged. Inlet control is commonly associated with shorter, steeper culverts with a free outfall downstream condition. When operating under outlet control the inlet configuration of a culvert continues to influence the head-discharge relationship; however, barrel characteristics such as roughness, area, shape and slope as well as the tail-water level contribute to the complexity of analysis. Outlet control is common for culverts with long rough barrels, low slopes and/or high tail-water conditions.

Over the years several authors/organisations (Chow, 1959; Bodhaine, 1976; French, 1985) have developed systems to describe and classify the possible combinations of flow regimes experienced by culverts. The characteristics used for these classification systems vary from author to author, however the main components often include: the head-water and tail-water levels, classification as mild or steep slope, and control location (inlet or outlet). An exhaustive review of past culvert research can be found in Day (1993), which contains summaries of significant culvert-related publications from 1911 to 1993. This literature review will therefore focus on recent developments in the field, and in particular to topics relating to the inlet region and fish passage through culverts.

2.1.2 Culvert Design

Traditionally, the primary goal of culvert design was to pass some selected design discharge underneath a roadway while maintaining a headwater elevation that would not result in overtopping of the roadway (Sturm, 2001). After the preliminary design determines the characteristics of the culvert (inlet configuration, slope, length, roughness, etc.) calculations are made to examine its head-discharge relationship under the full range of possible discharge conditions. These calculations can be made using a series of design charts and nomographs or using hydraulic modeling software such as HEC-RAS for unsubmerged conditions. The results of this analysis are then plotted as head vs. discharge and referred to as a performance curve. Other important issues regarding culvert design may include backwater effects, erosion control, safety, and fish passage.

As mentioned in Section 1.1, concerns regarding the ecological impact of culvert crossings have lead to changes regarding the philosophy and regulations concerning culvert design. In Canada, regulations related to fish passage fall under the jurisdiction of the *Fisheries Act* (Department of Fisheries and Oceans, 1985) and the Department of Fisheries and Oceans (DFO). The *Fisheries Act* section 20 (1), in essence states that the free passage of fish, must not, in the opinion of the Minister, be impeded by any obstruction or structure. This general requirement of free passage of fish has been further developed by numerous jurisdictions into specific design requirements and guidelines. In Manitoba, DFO and the Manitoba Department of Natural Resources have co-developed a document entitled *Manitoba Guidelines for the Protection of Fish and Fish Habitat* (Canadian

Department of Fisheries and Oceans and Manitoba Natural Resources, 1996). This document presents both recommendations and requirements relating to the design of culvert crossings. Requirements relating to the design of circular CSP culverts include:

- Average velocities should not exceed 0.8 m/s in culverts longer than 25 m and should not exceed 1 m/s in culverts shorter than 25 m. Velocities should not exceed the maximum prolonged swimming velocity of a fish regardless of length.
- Culverts should not result in any delay to migrating fish if spawning grounds are located immediately upstream of the crossing. There should be no delay to fish associated with the average annual flow. The crossing should not be impassable for longer than seven days relating to a flow rate with a one in fifty year return period.
- Water levels should not be greater than half of the pipe diameter during periods of fish migration.
- Culvert slopes should be maintained as close as possible to the natural stream grade.
- Culverts should be embedded a minimum of 30 cm or 10% of their diameter below the stream bed, whichever is greater. The length of the culvert should be backfilled with granular material up to the level of the natural stream bed.

2.1.3 Inlet Hydraulics

The hydraulic analysis of the inlet region can be separated into three zones. From upstream to downstream they are; the approach zone, an acceleration zone and a deceleration zone. Behlke *et al.* (1991), provides a theoretical description of culvert inlet hydraulics in a report entitled *Fundamentals of Culvert Design for Passage of Weak-Swimming Fish*, produced for the Alaskan Department of Transportation.

The approach zone, also referred to as the inlet pool by some authors, is made up of the region immediately upstream of the culvert inlet. The extent of the approach zone can be defined as, the length of channel upstream of the culvert inlet where flow patterns are not influenced by the culvert, with characteristics approaching fully developed open channel flow.

The cross-sectional area of a culvert is generally less than that of the stream within which it is installed. Therefore, to maintain continuity this reduction in area requires the velocity within the culvert to be greater than in the stream. The location at which streamlines begin to contract is the beginning of the acceleration zone. The increase in velocity comes from a shift of potential energy in the approach zone to kinetic energy within the acceleration zone resulting in a dip in the water surface. The shape of the culvert inlet can also influence the required increase in kinetic energy. If the required contraction is large and/or the edge of the inlet is sharp, flow will separate from the walls of the culvert creating an ineffective flow area immediately within the inlet of the culvert. According to the observations of Behlke *et al.* (1991), the effective flow area within the contracted section of the inlet is approximately three quarters of the flow area downstream in the culvert barrel. The report states that the magnitude of the contraction can be significantly reduced with the addition of a headwall to the inlet and nearly eliminated if the edge of the culvert is bevelled.

Once the flow has reached some maximum level of kinetic energy, streamlines will begin to diverge and make use of the full flow cross section. As the effective flow area expands and velocities decrease there is an additional energy loss. This energy is supplied via the potential energy of the approach zone.

2.2 Fisheries Considerations

2.2.1 Fish Passage

Numerous authors and publications (Behlke *et al.,* 1991; Federal Highway Administartion, 2001; Federal Highway Administration, 2007), have outlined why the consideration of fish passage is an important component of culvert design and how culverts may present a barrier to fish movements.

Fish require several types of habitat to complete their lifecycle including forage, spawning, nursery, and overwintering (Federal Highway Administration, 2007). The construction of culvert crossings can lead to the fragmentation of these habitats. If fish passage considerations are not incorporated into culvert design some of these habitats may be made inaccessible. Barriers to fish passage presented by culverts may include; excessive velocities, drops or perched outlets, debris accumulations, insufficient flow depths, and excessive turbulence.

There are several measures of velocity commonly referenced in regards to culvert fish passage. These are: point velocity, boundary layer velocity, and average velocity. Point velocity, refers to the instantaneous three dimensional velocity at any point within the culvert, often used to describe the velocity experienced at the nose of a fish. The boundary layer velocity, refers to the low velocity area adjacent to the water-culvert boundary. The existence of the boundary layer is related to the no slip boundary condition which states that the velocity of a fluid in contact with a stationary boundary must be zero. Streamwise velocities increase with distance from the boundary to some maximum. Generally, the rougher the boundary, the larger the low velocity area. Several authors have suggested that this lower velocity region may offer a means of passage for fish traveling up culverts (Ead et al., 2000; Kehler, 2009; Magura, 2007). The average cross sectional velocity or average velocity, refers to the flow rate within the culvert divided by the area of the flow cross section. The average velocity is often used in assessing fish passage conditions within a culvert due to its relative ease of calculation.

Drops or perched outlets can present a barrier to fish passage in that they will be impassable to any species and life stages of fish without the ability or motivation to clear excessive heights. Some species of fish possess the ability to jump out of the water to clear an obstacle; however this ability varies greatly with species and life stage (Federal Highway Administration, 2007). Stuart (1962) lists drop height, plunge pool depth, stream width (at drop), and light intensity as factors affecting the jumping ability of various species. Brandt *et al.* (2005), found that drop height and total length of fish were the most significant factors affecting the jumping performance of Brook Trout (*SalvelinusFontinalis*).

Insufficient flow depths present a barrier to fish passage. Fish require some minimum depth of flow for numerous reasons, including; to avoid oxygen starvation, to allow for them to create maximum thrust, and to avoid injury due to contact with the bed (Federal Highway Administration, 2007). As with other parameters, the minimum required depth is dependent on the species and life stage of fish.

A significant gap in the literature exists in the understanding of how fish respond to turbulence within a barrier. However, several authors report that excessive levels of turbulence can dissuade fish from entering or traversing a culvert if levels are enough to confuse their sense of direction and that some fish prefer to hold in areas of low turbulence (Federal Highway Administration, 2007). Smith *et al.* (2006), reported that in a controlled flume study, the density (holding location) of Rainbow Trout (*Oncorhynchus Mykiss*) could be correlated to turbulence and provided a functional measurement of the effects of discharge and cover. They found that fish would tend to hold at some moderate level of turbulence. Two measures of turbulence often referenced in the literature are; turbulent kinetic energy and energy dissipation factor. Pope (2000), describes turbulent kinetic energy (k) as a representation of the mean kinetic energy in a fluctuating velocity field where larger values represent increased turbulence or overall energy levels. Turbulent kinetic energy is a function of the root mean square of the instantaneous velocity (u'_i) the measure of variation in velocity at a point in relation to that point's time average velocity, essentially the standard deviation of velocity at a point (Nezu & Nakagawa, 1993).

$$u'_i = \sqrt{\overline{(u_i - U)^2}} \tag{2.1}$$

where:

- u_i $[m/s]$ is the instantaneous point velocity
- U $[m/s]$ is the time − averaged point velocity

Turbulent kinetic energy k [m^2/s^2] is then calculated as:

$$k = \frac{1}{2}\left(\sum {u'_i}^2\right) = \frac{1}{2}(u'^2 + v'^2 + w'^2) \tag{2.2}$$

Where:

- *u', v' and w'* $[m/s]$ are the three components of the root mean square velocity fluxuations

The energy dissipation factor (EDF) can used to quantify levels of turbulence over the full flow cross section of baffled culverts (Federal Highway Administration, 2007). EDF is a metric used to quantify the mean turbulent conditions within a structure used for fish passage. Maximum values of EDF are available for species common to costal regions;

however, less research has been conducted for inland/prairie species. Guidelines developed for Washington State recommend that EDF levels be maintained below 144-239 m-N/m^3/s within baffled culverts. EDF [m-N/m^3/s] is calculated as:

$$EDF = \gamma QS/A \tag{2.3}$$

Where:

- γ [N/m^3] is the unit weight of water
- Q [m^3/s] is the flow rate
- S [-] is the dimensionless slope of the culvert
- A [m^2] is the cross sectional flow area between baffles

The challenge presented to fish by each of these barriers is cumulative over the length of a culvert and conditions at the culvert inlet are the last to be overcome. Behlke *et al.* (1991) report observing fish navigate the outlet and barrel sections of a culvert only to encounter challenging inlet conditions, then eventually fatigue and be washed downstream.

2.2.2 Fish Swimming

Fish swimming is based on the use of two muscle systems, red and white, described in detail by Webb (1975) and numerous other authors. The red or aerobic muscle system is used for low-intensity, long-term movements such as traveling long distances or holding position in the current. The white or anaerobic muscle system is used for high intensity short term movements such as hunting or passing a velocity barrier. Heavy use of the white muscle system results in fatigue and requires significant rest to recover. Behlke *et al.* (1991), describes how red muscle output is a slow decaying function over time while white muscle output decays rapidly.

In an effort to quantify fish swimming abilities, researchers have developed a classification system for fish swimming based on the ability of a fish to maintain a velocity for some period of time. Bell (1986) outlines a classification of fish swimming into three modes: sustained, prolonged, and burst. Sustained swimming makes use of the red muscle system exclusively and can be maintained for hours, analogous to walking or slow jogging for human movement. When engaged in prolonged swimming, a fish uses a combination of the red and white muscle systems. Prolonged swimming speeds can be maintained for minutes, analogous to running for human movement. Burst swimming uses the white muscle system exclusively and can only be maintained for seconds, analogous to sprinting in human movement. The swimming ability of individual fish varies greatly and is strongly influenced by species and life stage.

The upstream movement of a swimming fish requires it to produce thrust greater than the forces it encounters in the current. These forces, as described by Behlke *et al.* (1991), include profile drag, gradient force, and virtual mass force. Profile drag is the force exerted by the fluid on the fish in the downstream direction and includes the effects of skin friction and pressure drag. For fish swimming within a turbulent boundary layer, profile drag F_d [N] can be calculated as:

$$F_d = \frac{0.072 b k \rho v^{0.2} L^{1.8} V_{fw}^{1.8}}{2} \qquad (2.4)$$

where:

- b [-] is a coefficient relating to the surface area of the fish, often close to 0.4
- k [-] is a constant between 3 and 5 depending on the fish and swimming conditions
- ρ [kg/m^3] is the mass density of water
- v [m^2/s^2] is the kinematic viscosity of water
- L [m] is the total length of the fish
- V_{fw} [m/s] is the swimming velocity of the fish with respect to the surrounding water

The gradient force F_g [N] is the force required by the fish to overcome gravity since it is traveling up hill. The gradient force is the resultant of the fish's weight and its buoyant force. The magnitude of the gradient force is dependant on the surrounding pressure gradient and its direction is normal to the slope of the hydraulic grade line.

For fish swimming in culvert-like conditions with slopes less than 6% and uniform flow, the gradient force can be calculated as:

$$F_g = WS \tag{2.5}$$

where:

- W [N] is the submerged weight of the fish
- S [-] is the slope of the culvert

The virtual mass force F_{vm} is the force required to maintain forward motion if it accelerates relative to the surrounding water. The force is in the direction opposite to the relative acceleration. The virtual mass force is of significant importance to fish passage at culvert inlets as there is often a large acceleration in flow velocity resulting from the reduction in flow area from stream to culvert. The virtual mass force can be calculated as:

$$F_{vm} = \frac{1.2 W a_{fw}}{g} \tag{2.6}$$

where:

- 1.2 is a multiplier accounting for the acceleration of the water within the boundary layer surrounding the fish
- g [m/s^2] is the acceleration due to gravity

- a_{fw} [m/s^2] is the relative acceleration of the fish with respect to the surrounding water

Behlke *et al.* (1991) also describe strategies employed by fish encountering these conditions at the inlet of a culvert. Depending on the species and life stage, fish may attempt to use the ineffective flow areas adjacent to the contraction zone to approach the inlet, if turbulence and velocities are suitable. If conditions are easy, or a fish's ability is high, it might challenge the contraction zone directly. Fish may also follow the bed making use of the lower velocity boundary layer.

2.3 Recent Culvert Fish Passage Studies

The significant cost associated with meeting regulatory requirements for culvert design has served as the motivation for several recent studies aimed at gaining a better understanding of the hydraulics of culverts as they relate to fish passage.

Ead *et al.* (2000) examined the velocity field in the fully developed region of a CSP culvert over a range of slopes and discharges. The study found that streamwise velocities near the boundary of the culvert were relatively small and that these low velocity regions may provide a corridor for fish passage. In their discussion of Ead et al., Papanicolaou & Talebbeydokhti (2002), recommended that three-dimensional analysis should be considered to gain an understanding of the secondary nature of the flow within culverts. They made the recommendation of examining spanwise and vertical velocity distributions as well as turbulent intensities and kinetic energy. Their response discussed the importance of these parameters to fish passage.

Magura (2007) performed a model study examining an embedded and backfilled CSP culvert with a projecting end inlet. The study included measurements of three-dimensional velocities throughout the length of the culvert. Notable findings included; the presence of relatively low streamwise velocities near the culvert boundaries and that the streamwise velocity distribution throughout the culvert was highly symmetrical about the center.

Tullis *et al.* (2008) examined entrance loss coefficients and head discharge relationships for embedded culverts designed for fish passage. The study found that inlet loss coefficients for buried inlet culverts were generally greater than for the same inlet geometry without inlet burial. The study also found that experimental inlet loss coefficients varied greatly with degree of submergence while culverts operated under un-submerged inlet conditions. Inlet loss coefficients were consistently greater for submerged than for un-submerged inlet conditions.

Abbs *et al.* (2007) examined the hydraulics of culverts operating under backwater conditions. This study examined velocity and turbulence intensity distributions within a CSP culvert under several discharge and backwater conditions. Their analysis found that creating a backwater effect would increase the size of low-velocity boundary zones. Their work also found that turbulence intensities were highest near the boundaries of the culvert, and that streamwise velocity distributions within the culvert were largely symmetrical about the center.

Day (1993) studied the turbulent flow field in the approach zone of a pipe culvert with a vertical headwall. This study examined streamwise and vertical velocity distributions as well as turbulence intensities. The study found that at a distance greater than 2.5 diameters upstream of the inlet, velocity and turbulence intensity profiles were unaffected by the inlet. The study also found that as flow approached the inlet, velocities increased and turbulence intensities decreased.

Chapter 3

Laboratory Setup

3.1 Laboratory Facilities

The physical model testing for this research study was conducted at the University of Manitoba's Hydraulics Research and Testing Facility (HRTF). The model employed in the study was originally used by Kehler (2009) and was modified to meet the objectives of this study. Water was circulated through the model using the laboratory's integrated distribution system. The distribution system consists of a constant head tank supplied with water from an underground reservoir by two pumps (65 hp and 75 hp). Water was delivered to the model from the constant head tank via a 350 mm diameter PVC supply line.

A coordinate system for the study was established with the x or streamwise direction defined along the length of the culvert with the positive axis in the direction of flow. The y or vertical direction was set with the positive axis upward. The z or spanwise direction orientated horizontally perpendicular to the flow with the positive direction defined to the left when looking in the positive x-direction.

3.2 Model Design and Construction

The model used for the study was designed to be representative of typical Manitoba culvert stream crossings. The design was based on drawings provided by Manitoba Infrastructure and Transportation.

3.2.1 Similitude and Scaling

The tests conducted for this study maintained a free surface along the length of the model and were conducted with completely rough flow regimes (roughness Reynolds number Re* > 70). As such the hydraulics of the modeling were dominated by gravitational forces and Froude model scaling was used in determining the model to prototype scaling factors.

$$F_m = F_p \tag{5.1}$$

$$\left(\frac{V_r}{\sqrt{g l_r}}\right)_m = \left(\frac{V_r}{\sqrt{g l_r}}\right)_p \tag{5.2}$$

Where F_m [-] is the Froude number of the model, F_p [-] is the Froude number of the prototype, V_r [m/s] is a representative velocity, l_r [m] is a representative length and g [m/s^2] is acceleration due to gravity. This relationship can be manipulated to determine the scaling factors associated with this study, several of which are presented in Table 3-1: Scaling Factors. As the model used for the study represents a generic crossing design the results were not converted to a prototype scale and remain as measured.

Table 3-1: Scaling Factors

Parameter	Scaling Factor
Length	λ
Area	λ^2
Velocity	$\lambda^{1/2}$
Discharge	$\lambda^{5/2}$

3.2.2 The Culvert

The culvert used for this study was a corrugated steel pipe with a diameter of 0.8 m, corrugation amplitude of 13 mm and a wavelength of 68 mm. The corrugations of the culvert used in this study were annular, as is typical of large diameter culverts. Annular corrugations were used because at a diameter of 0.8 m the angle of helical corrugations to the flow direction would have been significant and may have resulted in rotational flow. In large diameter culverts, the angle between the flow direction and corrugations is very small and therefore was assumed to not cause rotational flow. The culvert was made up of five 4.27 m long sections connected with corrugated steel couplers, resulting in a total length of 21.35 m. The seams and rivets of the culvert were sealed using an industrial polyurethane sealant to minimize leakage. To allow for sampling within the culvert access holes were cut at regular intervals along its length.

Figure 3-1: Culvert Model

3.2.3 Support System

The culvert was installed on 18 wooden saddles supported by threaded steel rods. The slope of the culvert was adjusted by raising or lowering the saddles on the threaded rods. The system allowed the slope of the culvert to be set between 0% and 1.5%.

3.2.4 Headwater and Tailwater Tanks

Headwater and tailwater tanks were constructed at the upstream and downstream ends of the culvert using standard dimensional lumber and high density plywood. The seams of the tanks were sealed using an industrial polyurethane sealant to minimize leaks. The headwater tank was constructed with a length and width of 4.5 m and 2.75 m, respectively. The width of the headwater tank resulted in a width-to-diameter ratio of 3.4. The length of the headwater tank was selected to allow sufficient space for flow to pass a flow straightener and stabilize prior to reaching the culvert inlet. The headwater tank was constructed with 1 m of the culvert projecting within the inner wall. The headwater tank and culvert were connected using an adjustable rubber gasket. The various inlet treatments used for the study were installed within the headwater tank. The tailwater tank was constructed with 1 m of the culvert projecting within its inner wall and incorporated a flap gate used to regulate the downstream water level.

3.2.5 Inlet Treatments

Three inlet treatments were developed for this study based on standard designs provided by Manitoba Infrastructure and Transportation. A vertical headwall, a 45° wingwall and a projecting end inlet were constructed of standard dimensional lumber and plywood. The inlets were installed within the headwater tank.

The vertical headwall inlet treatment (Figure 3-2) consisted of a vertical wall mounted flush with the lip of the culvert and perpendicular to the bed of the headwater tank. The

45° wingwall inlet treatment (Figure 3-3) used the same vertical wall with the addition of vertical wingwalls extending from the edge of the culvert to the walls of the headwater tank at 45°. The projecting end inlet treatment (Figure 3-4) extended from the bed of the culvert at a slope of 3:1 horizontal to vertical and intersected the lip of the culvert at 0.1 diameters (8 cm) above its invert.

Figure 3-2: Vertical Headwall

Figure 3-3: 45° Wingwall

Figure 3-4: Projecting End Inlet

3.2.6 Gravel Bed Material

In an effort to simulate a field culvert installation the approach zone of the headwater tank was lined with crushed limestone. Non-embedded tests of each inlet treatment were conducted with the headwater tank backfilled with crushed rock up to the invert of the culvert. The embedded test condition was conducted with an additional 0.1 diameters (8 cm) of material added to the headwater tank.

The backfilled test condition was conducted with 0.1 diameters (8 cm) of crushed rock placed throughout the length of the culvert (Figure 3-5). Plywood baffles (Figure 3-6) were installed approximately every 0.25 meters below the level of the gravel to avoid significant amounts of flow within the rock and represent a mature silted culvert installation. The material used for the study was selected based on specifications provided by Manitoba Infrastructure and Transportation. The d_{50} of the material was 2.76 cm and its gradation was relatively uniform.

Figure 3-5: Projecting End Backfilled Inlet Configuration

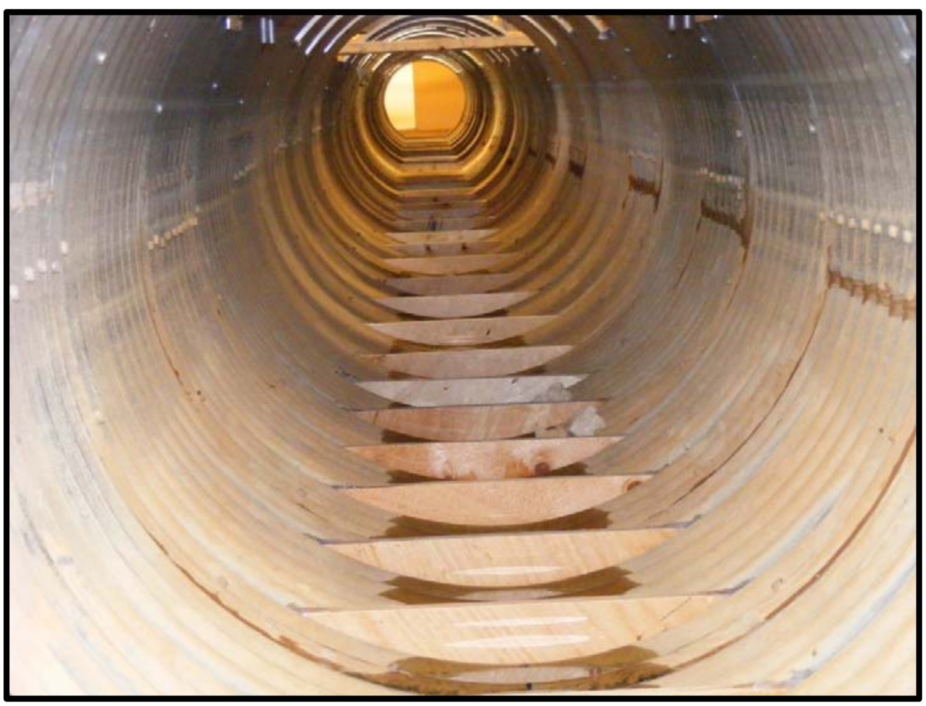

Figure 3-6: Plywood Baffles

3.3 Sampling Equipment

3.3.1 Discharge Measurement

Discharge through the model was measured using an MSR Magnum Standard Magmeter installed in the water supply pipe. The magmeter was installed according to the manufacturer's instructions within the longest straight section of the supply pipe available. The accuracy of the magmeter is listed by the manufacturer as 0.5% of the average velocity. Measurements from the magmeter were output to a PC and recorded using a LabVIEW® software system originally developed by and outlined in Kehler (2009). The output of the magmeter was periodically verified using the laboratory's integrated volumetric discharge measurement system.

3.3.2 Motion Control System

In an effort to automate the sampling procedure the motion control system developed by Kehler (2009) was modified to meet the needs of this study. The motion control system consisted of a two-axis servo motor motion system controlled by a LabVIEW interface. The motion control system synchronized the movements and sampling of the various instrumentation and allowed them to be positioned precisely within the flow field. For tests within the inlet region of the culvert the motion control system was attached to a levelling platform and could be positioned manually at any cross section within that range (0.25 to 1 diameters downstream of the inlet). Positioning and setup of the motion control system were simplified by referencing the movements of the ADVs relative to the invert of the culvert, located using the 'Boundary' command of the downward looking ADV. It was therefore not necessary to adjust the vertical position of the motion control system as it was moved along the length of the culvert. For tests conducted at two diameters downstream of the inlet the motion control system was attached to the levelling platform described in Kehler (2009).

3.3.3 Depth Measurements

Water surface profiles along the length of the culvert were measured using a series of manometers installed along the bed of the culvert. In total 28 manometers were installed, including one in both the headwater and tailwater tanks. To facilitate water surface profile measurements, taps were set into the bed of the culvert at regular intervals and connected via clear flexible tubing to three separate manometer clusters. Each cluster was surveyed to a common datum and readings were entered into a standardised EXCEL spreadsheet. Where water depths were required between manometer locations an acoustic level gauge was used, mounted to the motion control system.

3.3.4 Velocity Measurements

Velocity measurements were recorded using three orientations of SonTek acoustic Doppler velocimeters (ADVs). ADVs measure three dimensional velocity components of particles entrained in flow using a principle known as the Doppler shift. The Doppler shift principle is based on the change in frequency of a signal reflected by an object in motion relative to the source/receiver. ADVs operate by emitting sound waves from a central excitation transmitter; reflections of these sound waves are then recorded by three receivers surrounding the transmitter. The alignment of the receivers is such that reflections are recorded from a specific remote sampling volume. The ADV measurement technique can therefore be referred to as quasi-non-invasive as the instrument is submerged in the flow but does not contact the measured sampling volume. The size of the sampling volume varies with the model of ADV. Three dimensional velocities of the entrained particles are then calculated based on the frequency shift between the transmitted and recorded signals. The assumption is made that the measured velocity of the entrained particles is equal to the water velocity.

The orientations and models of ADVs used in this study were a downwards looking SonTek 16 MHz MicroADV, an upwards looking SonTek 16 MHz MicroADV, and a side looking SonTek 10MHz ADV. The sampling volume of instruments was 0.09 cm^3 for the 16 MHz MicroADVs and 0.25 cm^3 for the 10 MHz ADV. The 16 MHz MicroADVs were capable of recording measurements at a rate of 50 samples per second while the 10 MHz ADV was limited to 25 samples per second. The smaller sampling volume and faster sampling rate of the 16 MHz MicroADVs made them the preferred instrument, and use of the 10 MHz ADV was limited to regions of the flow field that the 16 MHz MicroADVs could not access. For each ADV model the center of the sampling volume is located 5 cm from the probe.

Chapter 4

Testing Procedure

4.1 Experimental Plan

The experimental plan for this study was developed based on the findings of previous culvert model studies as well as the findings of preliminary testing conducted as part of this work. As tests were time consuming both to setup and conduct, it was important to focus efforts on the most valuable scenarios. The experimental plan was developed to meet the objectives outlined in Section 1.2 of this thesis.

Magura (2007) found that the slope of the culvert did not significantly affect the flow structure within the inlet region. Based on this finding, it was decided that tests would be conducted at a slope of 0.26%. It was felt that this slope would be representative of the typical low slope culvert installations in the Canadian Parries while not limit the usefulness of the results to other regions. Magura (2007) also found that the structure of the flow field within the inlet region was similar regardless of the flow rate. This was confirmed as part of the preliminary testing conducted for this research. Based on these criteria, it was determined that the majority of tests would be conducted at a flow rate of 0.175 cms, corresponding to the high flow rate condition examined by Kehler (2009).

Tests were conducted with each of the three inlet treatments described in Section 3.2.5. The projecting end inlet treatment was also tested with the culvert embedded 0.1 diameters (8 cm) below the model stream bed and with the embedded culvert backfilled with 0.1 diameters (8 cm) of gravel. Non-embedded tests were conducted with the downstream water level set to the culvert normal depth, following the methods developed by Kehler (2009). In an effort to simulate the effects of installing a culvert below the stream bed, the embedded and embedded- backfilled tests were conducted with the tailwater raised by 0.1 diameters (8 cm) above the normal depth of the no-gravel condition resulting in a slight M1 profile.

4.2 Data Collection

4.2.1 Longitudinal Water Surface Profiles

The first dataset recorded for each test condition was the water surface profile along the length of the culvert. The longitudinal water surface elevations were measured by recording the levels of the manometers installed along the base of the culvert. Measurements of the flow depth within the headwater and tailwater tanks were also recorded. This data was then compared to a survey of the culvert invert to calculate the flow depth along the length of the culvert. The calculated water depths were plotted along with the expected normal depth and used to ensure the proper downstream gate setting was in place. The recorded water depths within the inlet region were also set as the upper boundary in development of the motion control command files used for the velocity tests. The calculated water depths made it possible to calculate the entrance loss associated with each inlet configuration. Calculated inlet losses will assist in the comparison between the inlet configurations used for this work and other studies as well as field installations.

4.2.2 Horizontal Water Surface Profiles

Magura (2007) discusses a 'mounding effect' at the water surface associated with the plunging and contracting flow near the immediate inlet of his projecting end inlet culvert model. This horizontal water surface profile was also observed with each of the inlet configurations used in this study. In an effort to gain a better understanding of the complex structure of the water surface within the inlet region, horizontal water surface profiles were recorded for each of the four cross section locations for each inlet configuration. To facilitate these measurements the acoustic level gauge was mounted to the motion control system and used to record the flow depth at 2.5 cm intervals. The recorded water depths within the inlet region were then used to set the upper boundary in development of the motion control command files used for the two dimensional cross section testing.

4.2.3 Cross Section Velocity Measurements

In an effort to gain a detailed understanding of the flow structure within the inlet region, point velocity measurements were recorded using the three orientations of ADV described in Section 3.3.4. Three orientations of ADV (up, down and side-looking) were required to sample the full cross section of the velocity field and to sample in close proximity to the boundary of the culvert.

Based on the description of culvert inlet hydraulics found in Behlke *et al.* (1991), the findings of Magura (2007), and preliminary testing completed for this study, it was decided that detailed velocity testing would focus on the region located between the inlet and a downstream distance of two diameters. This location was chosen because the complex aspects of the inlet flow field occur within this range. After two diameters the flow field becomes similar to the fully developed region examined extensively by Kehler (2009) and others. Within the inlet region, cross sections at 0.25, 0.5, 1 and 2 diameters downstream from the inlet were set as the measurement locations. Velocity measurements were recorded at these four locations for each of the inlet configurations resulting in a total of 20 cross section datasets.

Magura (2007), Abbs *et al.* (2007) and others have reported in previous culvert studies that the flow field within culverts is symmetrical about the center. Based on these findings and following the approach adopted by Kehler (2009) flows were assumed to be symmetrical and measurements were only collected for one half of the flow field. The assumption of symmetry allowed point measurements to be recorded with an increased density without significantly increasing the duration of tests.

Kehler (2009) recorded point velocities within the fully developed region along radials emanating from the center of the culvert. This testing pattern was adopted to facilitate the development of empirical equations describing the streamwise velocity field. Initial testing demonstrated that a radial testing pattern failed to capture the complex nature of the flow field within the inlet region. As part of the initial testing program various grid sampling patterns were examined with spacing ranging from 2.5 cm to 10 cm. An offset diamond grid pattern with a spacing of 2.5 cm horizontal and 5 cm vertical was found to offer the best economy between level of detail and testing time. At each point location 12,000 instantaneous velocity samples were collected and used to calculate the average three dimensional point velocity as well as turbulence quantities. As outlined in Kehler (2009), the sampling duration for point measurements was determined so as to allow for the calculation of turbulence quantities within 2% of the long term value (greater then 30,000 samples).

4.3 Data Processing

4.3.1 Data Collection and Organization

To facilitate post processing, data collected for each inlet treatment was stored within a standardized folder structure. For each inlet treatment, a main folder was created containing sub-folders associated with each cross section location. The cross section folders each contained eight sub-zone folders used to keep the duration of each test reasonable. This was required to maintain an accurate water temperature reading for each test as well as to accommodate other testing programs underway in the laboratory. The sub-zone folders contained a folder associated with the up, down and side-looking ADVs. The ADV folders contained the motion control files and were the storage location for the raw ADV data files. During testing, output data was recorded as ASCII text files containing ten columns of data for each of the 12000 measurements recorded at each point. The first column of data corresponded to the sample number, columns two through four are the streamwise, spanwise and vertical velocity, columns five through seven are the recorded amplitude and the last three columns are the recorded correlation. The last row of data in each raw data file is the position of the sampling volume output by the motion control system.

4.3.2 Data Filtering

Raw ADV files were processed using two MATLAB scripts adapted and modified from those used by Kehler (2009). These scripts were used to ensure the quality of the data and to facilitate further analysis.

The initial step in post processing was to run the data through a script referred to as 'Data Cleanup'. The input to this script was the sub-zone folder containing the raw ADV data files recorded during testing. The first component of 'Data Cleanup' involved the removal of erroneous data spikes using a phase space filter algorithm developed based on the work of Goring & Nikora (2002). The data spikes are associated with the aliasing of the Doppler signal and can be caused by flow velocities outside the preset sampling range or through contamination of acoustic signals by the reflection of a previous pulse. The de-spiking algorithm is based on the premise that 'good' velocity data will cluster when plotted in phase space (a three dimensional plot of u_i vs. du_i/dt vs. d^2u_i/dt^2). Data points outside of this cluster are determined to be spikes and are removed.

After the de-spiking algorithm has run, the script calculates the average point velocity, turbulence intensity, second order turbulence quantities, signal to noise ratio (SNR), and the correlation score (COR) for each point location.

The SNR and COR are then used as an additional quality check for the point data. Points with a SNR of less than 15 dB and a COR of less than 50% are rejected. The rejection thresholds were selected based on recommendations found in SonTec (2001) and are described in detail by Kehler (2009). The final step of the 'Data Cleanup' script is to save the processed data of each testing zone into a .mat file containing the original data, processed data and a summary of key test parameters.

The second post processing script used to prepare the data for analysis was referred to as 'tecplot2Dfile'. This script was used to calculate the turbulent kinetic energy (k) and to normalize data within the .mat files by an appropriate parameter.

Spatial data were normalized by the culvert diameter (0.8 m), velocity data were normalized using the average streamwise velocity within the fully developed region of the culvert corresponding to the normal depth of non-embedded/backfilled configurations, *k* was normalized by the squared average streamwise velocity (U_{avg}^2) within the fully developed region of the culvert.

In addition, the 'tecplot2Dfile' script was used to combine the normalized data for each testing zone into a single text file containing all of the data associated with a cross section and test condition. Text files were formatted to comply with a standard TecPlot 360® layout and facilitated the development of figures and the analysis outlined in the following chapters.

Chapter 5

Results and Analysis

5.1 Introduction

This section present the analysis and results of the testing program carried out for this study. Table 5-1 provides a summary of the key hydraulic parameters associated with the various inlet configurations and testing locations. The recorded water surface profiles and calculated entrance losses associated with each test configuration are examined in Section 5.2, with the aim of developing a general understanding of the hydraulic conditions within each of the five inlet configurations. Sections 5.3 and 5.4 present the primary focus of this study, cross-section datasets of normalized velocity and turbulence data developed using the procedure described in Chapter 4. Cross-section datasets were developed for each inlet treatment at each measurement location to facilitate the visual and numerical comparison of conditions within the inlet region as well as between inlet types. The two dimensional datasets were plotted and analysed using the TecPlot 360® software package.

Table 5-1: Hydraulic Parameters

Inlet Treatment	Location	Depth	Area	U_{avg}	F	Re
[-]	[D]	[m]	[m²]	[m/s]	[-]	[-]
Vertical Headwall	0.25	0.365	0.223	0.785	0.474	147487
	0.5	0.364	0.223	0.785	0.474	147737
	1	0.382	0.237	0.738	0.433	143369
	2	0.391	0.244	0.717	0.415	141284
45° Wingwall	0.25	0.3749	0.231	0.758	0.450	145059
	0.5	0.3822	0.237	0.738	0.433	143322
	1	0.3795	0.235	0.745	0.438	143960
	2	0.3846	0.239	0.732	0.428	142760
Projecting End	0.25	0.3624	0.221	0.792	0.480	148139
	0.5	0.3613	0.220	0.795	0.483	148416
	1	0.3732	0.230	0.761	0.453	145470
	2	0.3843	0.239	0.732	0.428	142830
Projecting End Embedded	0.25	0.4063	0.256	0.684	0.386	137878
	0.5	0.4084	0.258	0.678	0.381	137423
	1	0.416	0.264	0.663	0.368	135801
	2	0.4233	0.270	0.648	0.356	134278
Projecting End Backfilled	0.25	0.417	0.302	0.580	0.295	135591
	0.5	0.417	0.302	0.579	0.294	135591
	1	0.425	0.308	0.567	0.284	133928
	2	0.437	0.318	0.551	0.271	131505

5.2 Water Surface Profiles and Entrance Losses

As with any hydraulic conduit, analysis of the energy grade line over the length of a culvert can provide valuable insight into the hydraulic conditions within the structure. The energy contained within culvert flow can be either potential (related to elevation and depth) or kinetic (related to velocity). Figures 5-1 through 5-5 present the recorded water surface plots normalized by the model culvert diameter (0.8 m). Calculated values of k_e and the culvert entrance loss coefficient are presented in Table 5-2.

Energy losses related to the contraction and expansion of flow within the inlet were determined by fitting a linear trend line to a plot of total head loss against distance, for manometer locations outside of the region influenced by the inlet (taken as greater than 3.5 metres downstream of the inlet). Under the employed test conditions, barrel velocities were maintained constant along the length of the culvert and therefore energy loss within this region were linear and associated with the roughness of the culvert. The energy loss associated with the inlet could then be reasonably approximated as equal to the intercept of the trend line with the vertical axis. The inlet head loss coefficient was then calculated as:

$$k_e = \frac{\Delta H}{\left(\frac{{U_{avg}}^2}{2g}\right)} \tag{5.1}$$

Where:

- ΔH [m] is the total head lost due to the contraction and expansion of flow within the inlet
- U_{avg} [m/s] is the average velocity in the culvert barrel downstream of the expansion zone

- g [m/s^2] is the acceleration due to gravity
- k_e [-] is an inlet loss coefficient based on the inlet geometry

Table 5-2: Inlet Loss Coefficients

Inlet Configuration	ΔH	U_{avg}	k_e
[-]	[m]	m/s]	[-]
Vertical Headwall	0.01030	0.722	0.388
45° Wingwall	0.00098	0.738	0.035
Projecting End	0.00920	0.738	0.331
Projecting End Embed-ded	0.01110	0.636	0.539
Projecting End Back-filled	0.02880	0.846	0.789

Entrance losses are greatest for the projected end backfilled configuration which corresponds to the work of Tullis *et al.* (2008), and their findings that burying a culvert results in greater inlet losses than found with the same geometry under non-backfilled conditions. The embedded inlet configuration also results in greater head loss than the non-embedded projecting end inlet. The smoothest entrance conditions are presented by the 45° Wingwall configuration with a calculated loss coefficient an order of magnitude less than the other configurations.

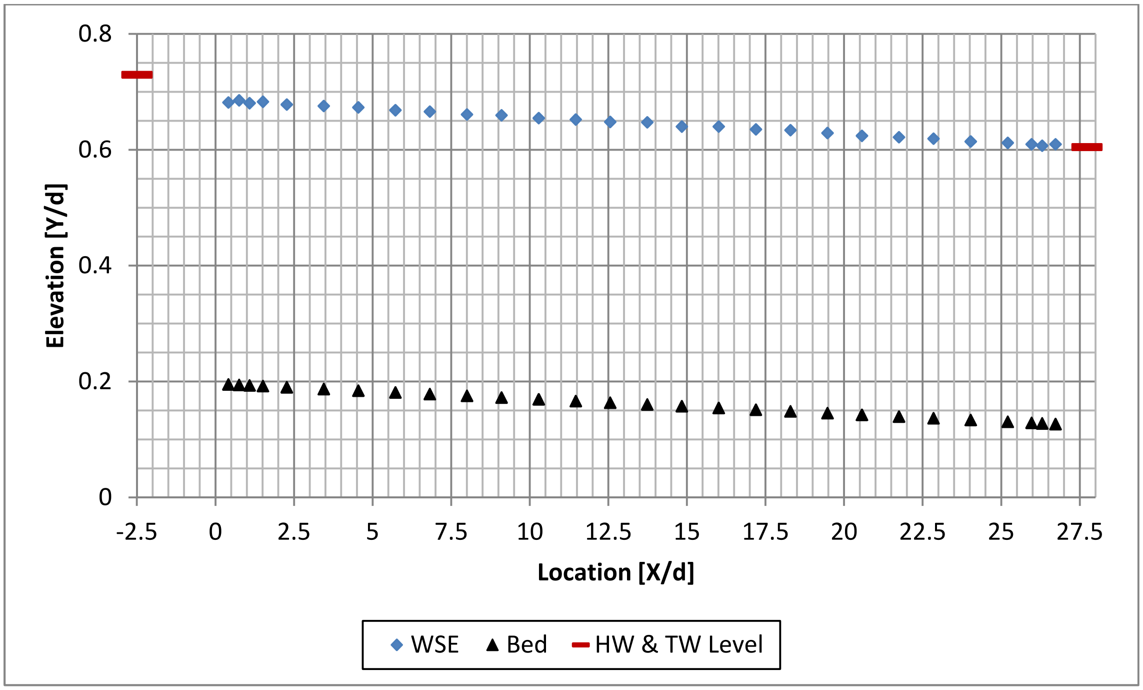

Figure 5-1: Water Surface Profile Vertical Headwall Inlet

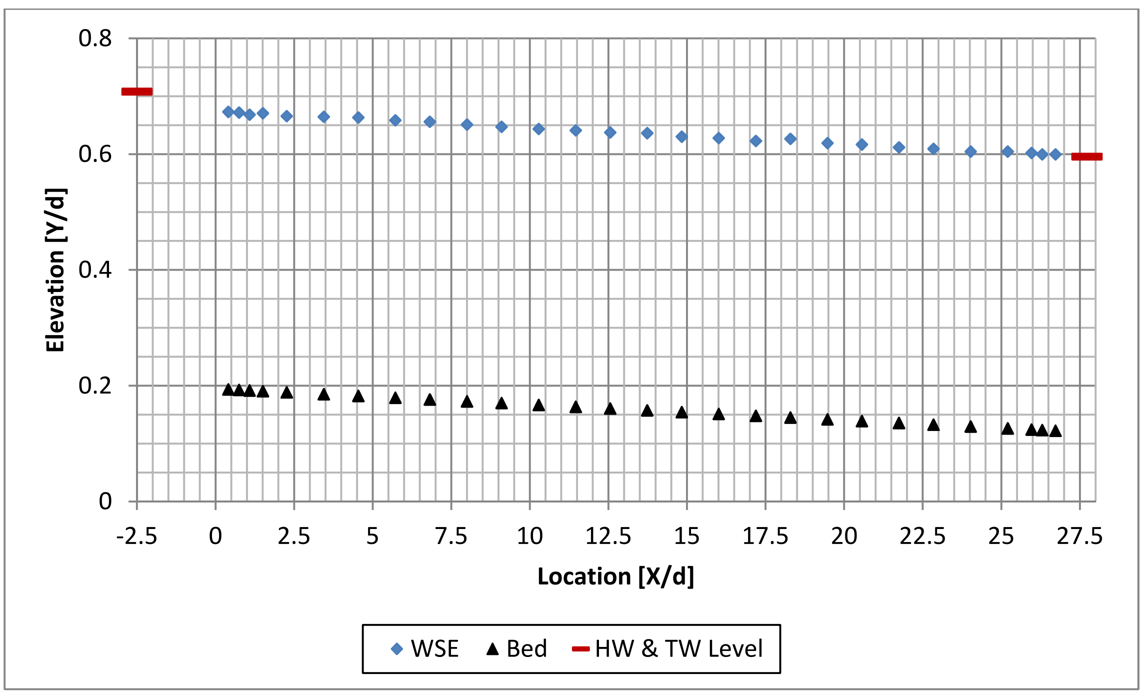

Figure 5-2: Water Surface Profile 45° Wingwall Inlet

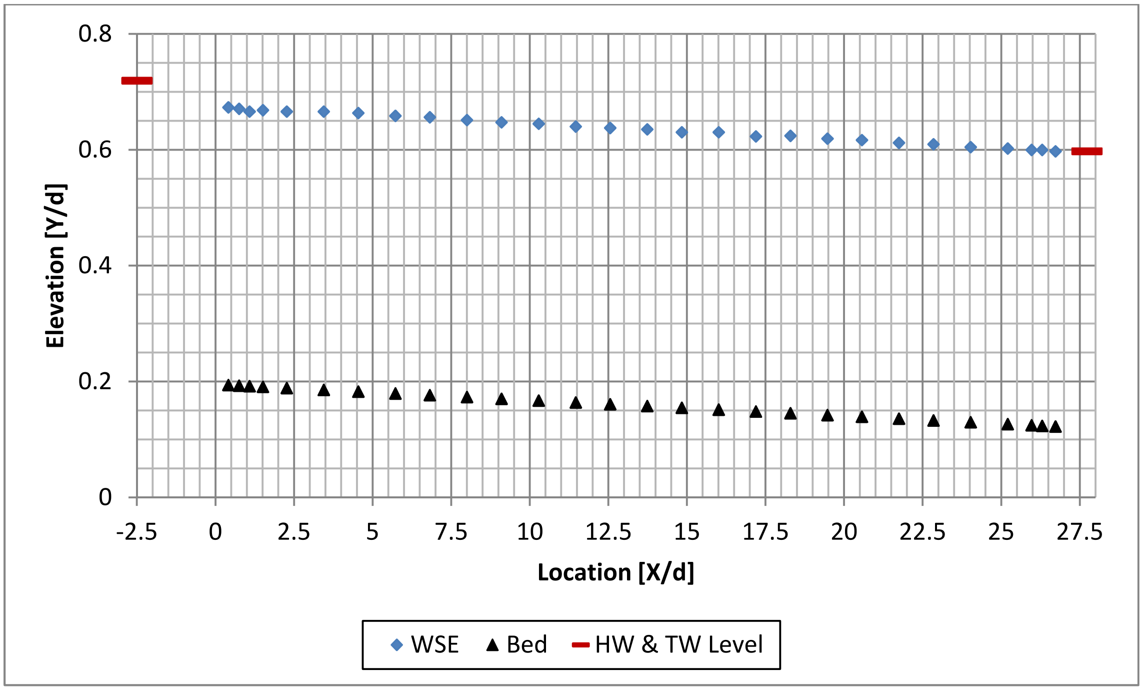

Figure 5-3: Water Surface Profile Projecting End Inlet

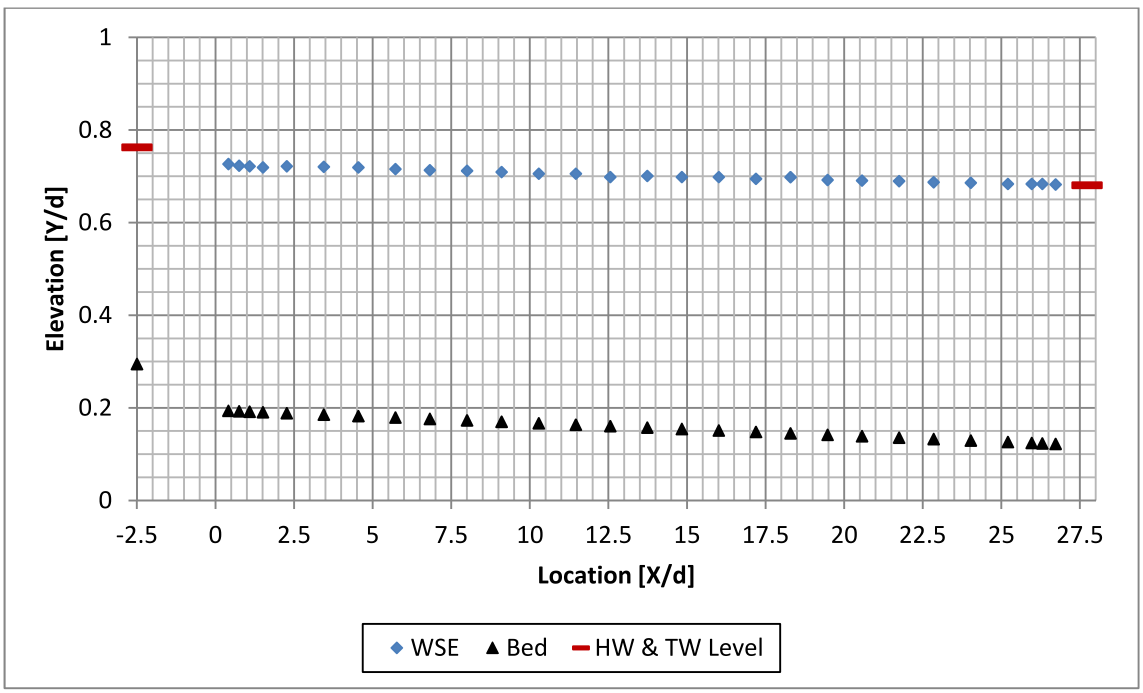

Figure 5-4: Water Surface Profile Projecting End Embedded Inlet Configuration

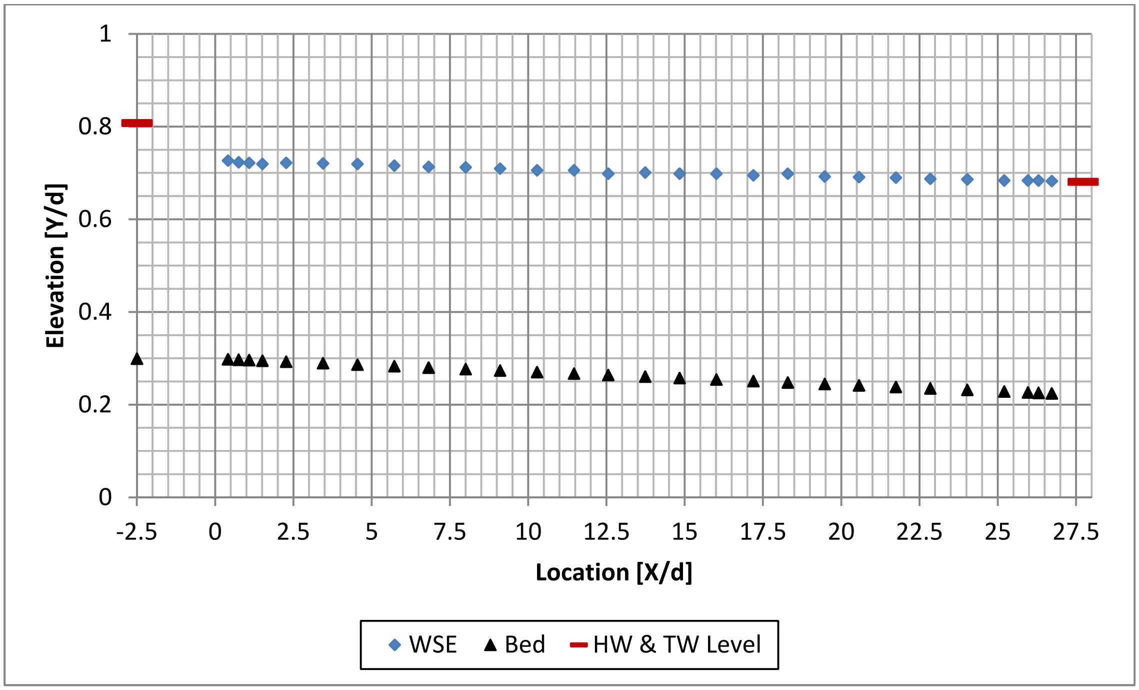

Figure 5-5: Water Surface Profile Projecting End Backfilled Inlet Configuration

5.3 Velocities

Figures 5-6 through 5-10 present isovel plots of the normalized streamwise velocities, as well as secondary velocity vectors of the normalized spanwise and vertical velocities for the various test conditions. The following paragraphs describe the flow conditions relating to each inlet treatment.

5.3.1 Vertical Headwall

At 0.25 diameters downstream of the inlet (Fig. 5-6a), pockets of low and negative streamwise velocity are present along the culvert boundary. A jet of high velocity flow is located at the center of the culvert surrounded by these low velocity zones. The width of the central jet is greater near the water surface. Of interest is the location of the maximum velocity, adjacent to the low velocity recirculation zone. There is a high velocity gradient between the low velocity zone and the central high velocity zone. Secondary velocity vectors at 0.25 diameters show the contracting and plunging flow resulting from accelerating water entering the culvert near the water surface. Secondary velocities are greatest near the boundary of the central jet and low velocity zone.

At 0.5 diameters (Fig. 5-6b) downstream of the inlet, the velocity gradient between the central jet and low velocity recirculation zone has diminished. A small region of negative streamwise velocity remains in the upper corner of the flow field. Secondary velocity vectors have diminished in magnitude and show that the flow is no longer contracting. Spanwise and vertical velocities are relatively negligible near the center of the jet.

Streamwise velocity isovels at a distance of one diameter downstream from the inlet (Fig. 5-6c) show that the shape of the central high velocity zone has inverted. At this location the width of the high velocity zone is greater near the bed than at the water surface. The location of the low velocity zone has become concentrated in the upper corner of the flow field and negative streamwise velocities are no longer present. The location of maximum velocity has shifted to the center of the culvert. The velocity gradient between high and low velocity zones has diminished further. Vectors of the spanwise and vertical velocities demonstrate the expansion of the central jet with water drawn from the lower portion of the high velocity zone into the low velocity zone. Spanwise and vertical velocities remain negligible near the center of the flow field.

At two diameters downstream of the inlet (Fig. 5-6d), the low velocity recirculation zone is no longer apparent as the flow field has now reattached to the boundary. Secondary velocity vectors show the continued expansion of the high velocity region, however the magnitudes have decreased.

a)

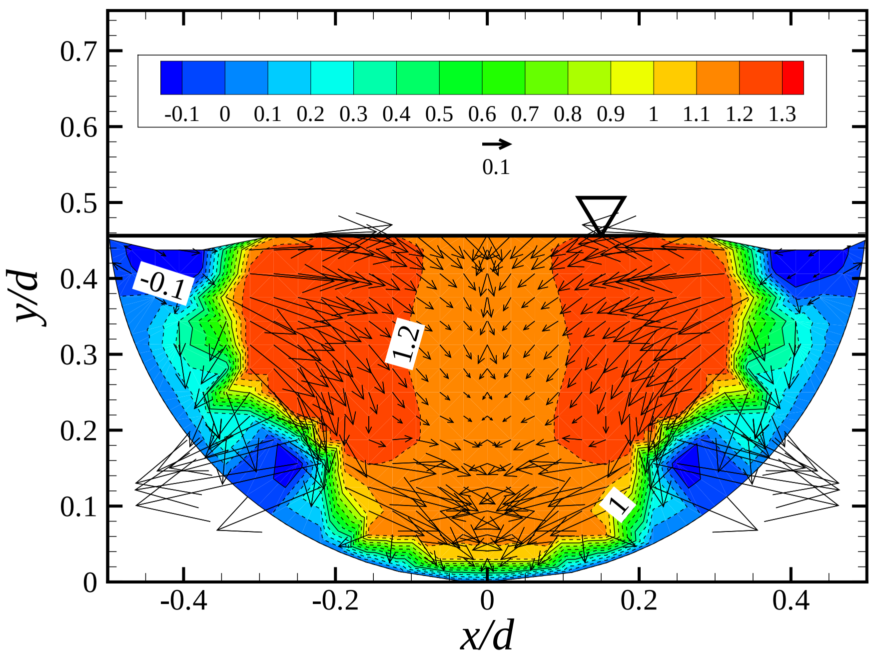

0.7
0.6
0.5
0.4
0.3
0.2
0.1
0
-0.1 0 0.1 0.2 0.3 0.4 0.5 0.6 0.7 0.8 0.9 1 1.1 1.2 1.3
0.1
-0.1
1.2
1
y/d
-0.4
-0.2
0
0.2
0.4
x/d

b)

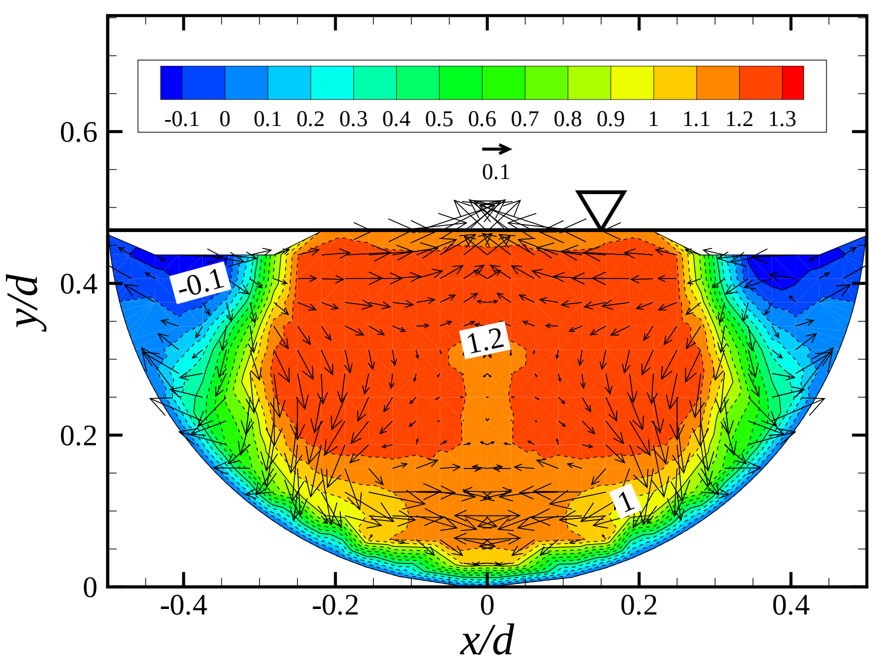

0.6
0.4
0.2
0
-0.1 0 0.1 0.2 0.3 0.4 0.5 0.6 0.7 0.8 0.9 1 1.1 1.2 1.3
0.1
-0.1
1.2
1
y/d
-0.4
-0.2
0
0.2
0.4
x/d

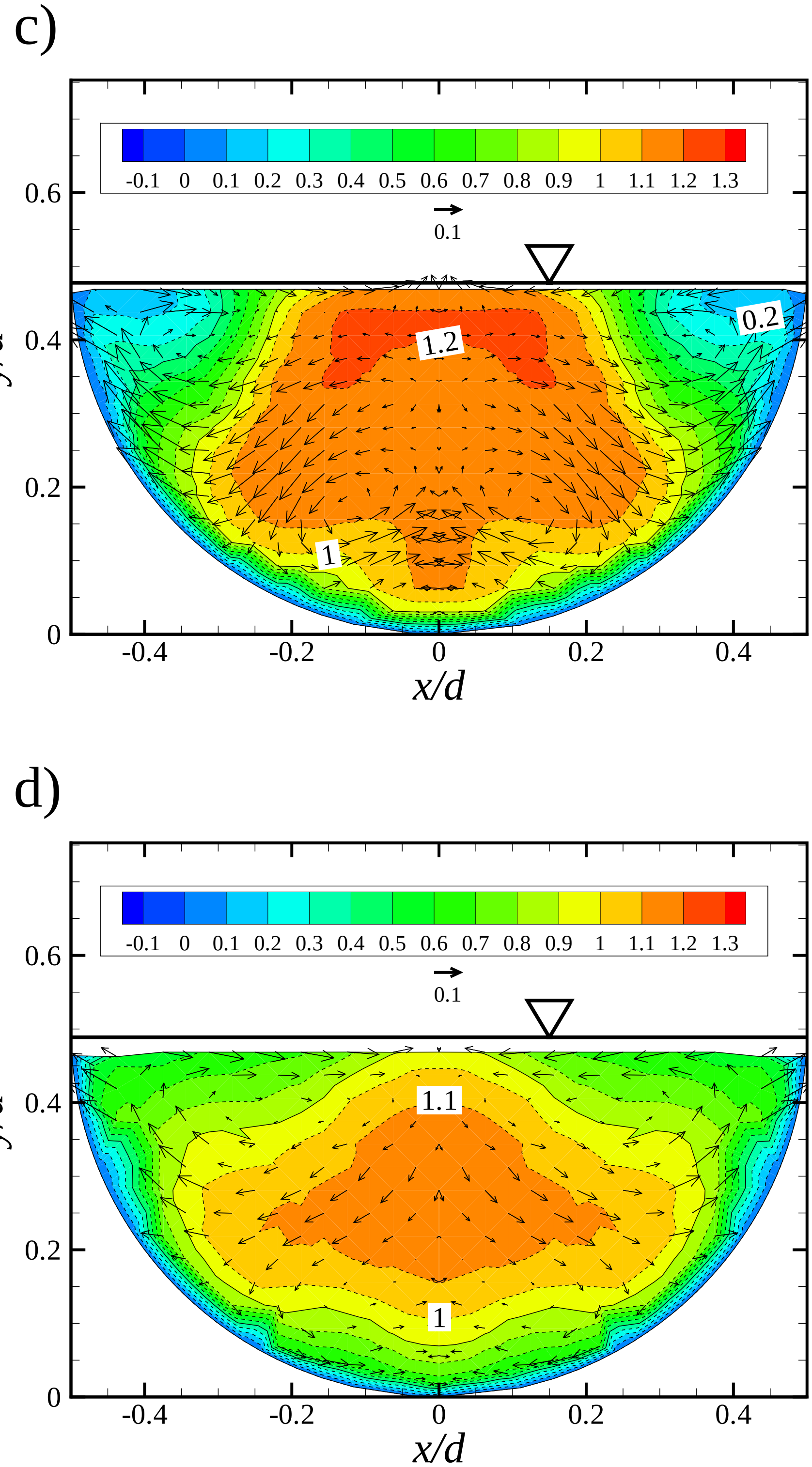

Figure 5-6: Distribution of U/U_{avg} and secondary velocity vectors for the vertical head-wall inlet treatment at a) 0.25D b) 0.5D c) 1D d) 2D

5.3.2 45° Wingwall

Isovel plots of normalized streamwise velocity at 0.25 diameters (Fig. 5-7a) show that at this location the flow has not separated from the boundary, indicating a smooth transition from the approach zone into the culvert inlet. The velocity field shows the maximum streamwise velocity offset from the center of the culvert flanking a significant area with velocities slightly above U_{avg}. Secondary velocity vectors show contracting and plunging flow with negligible magnitudes near the center of the culvert.

At 0.5 diameters (Fig. 5-7b), the flow is characterized by a central jet with velocities slightly above U_{avg} and a small recirculation zone in the upper corners of the flow field indicating flow has separated from the boundary. The velocity gradient adjacent to the recirculation zone is relatively mild. Secondary velocity vectors have diminished in magnitude and are negligible near the center of the flow field.

Velocity plots at one diameter (Fig. 5-7c), show that flow has reattached and the velocity gradient between the boundary and central region has become fairly mild. Low velocity regions are present at the sides of the flow field and the central jet has diminished in size. Secondary velocity vectors show the flow expansion and remain negligible at the center of the flow field.

At two diameters downstream of the inlet (Fig. 5-7d), velocity isovels show that the region of maximum velocity has become depressed below the water surface. The velocity gradient between the boundary and the high velocity region is mild. A significant portion of the flow field near the boundary and the water surface has streamwise velocities less than the average velocity. Secondary velocity vectors show the development of week spiraling secondary circulation currents.

a)

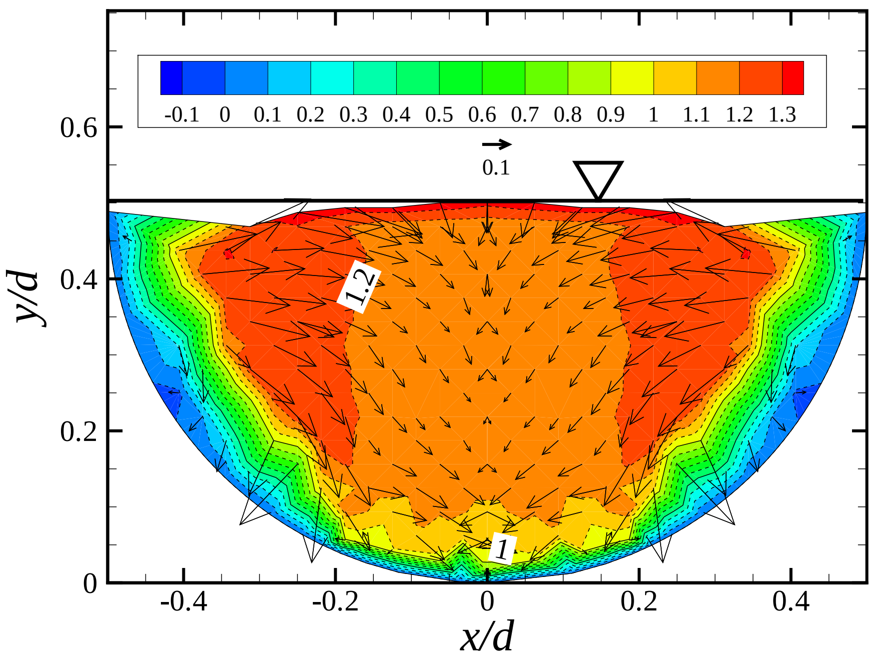
-0.1
0
0.1
0.2
0.3
0.4
0.5
0.6
0.7
0.8
0.9
1
1.1
1.2
1.3
0.1
1.2
1
y/d
x/d

b)

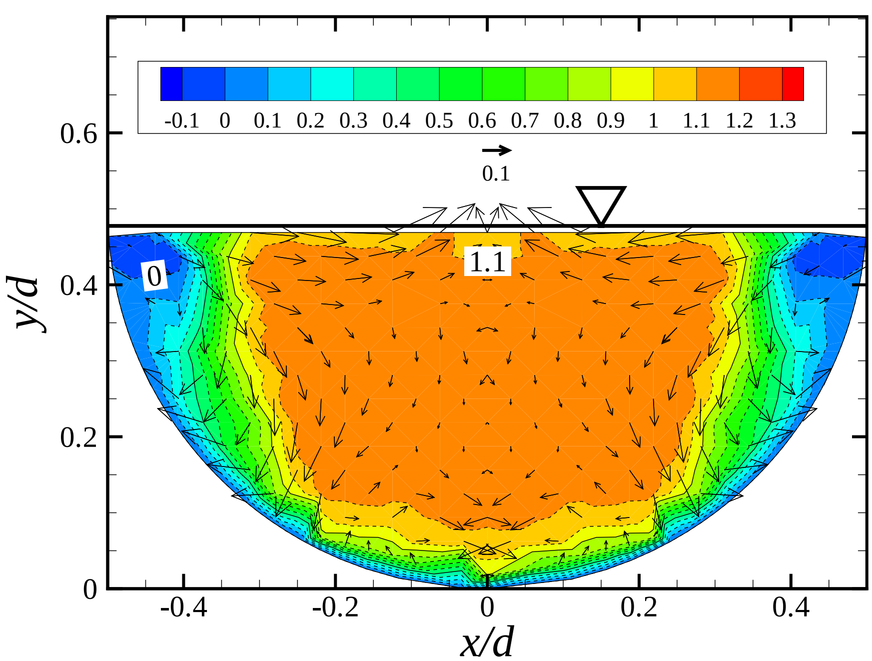
-0.1
0
0.1
0.2
0.3
0.4
0.5
0.6
0.7
0.8
0.9
1
1.1
1.2
1.3
0.1
1.1
0
y/d
x/d

c)

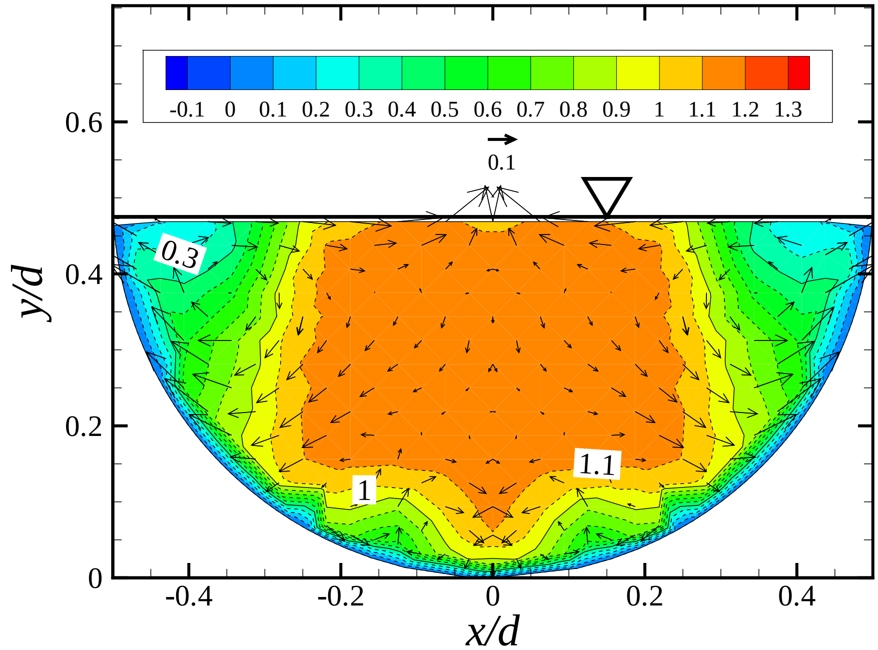

d)

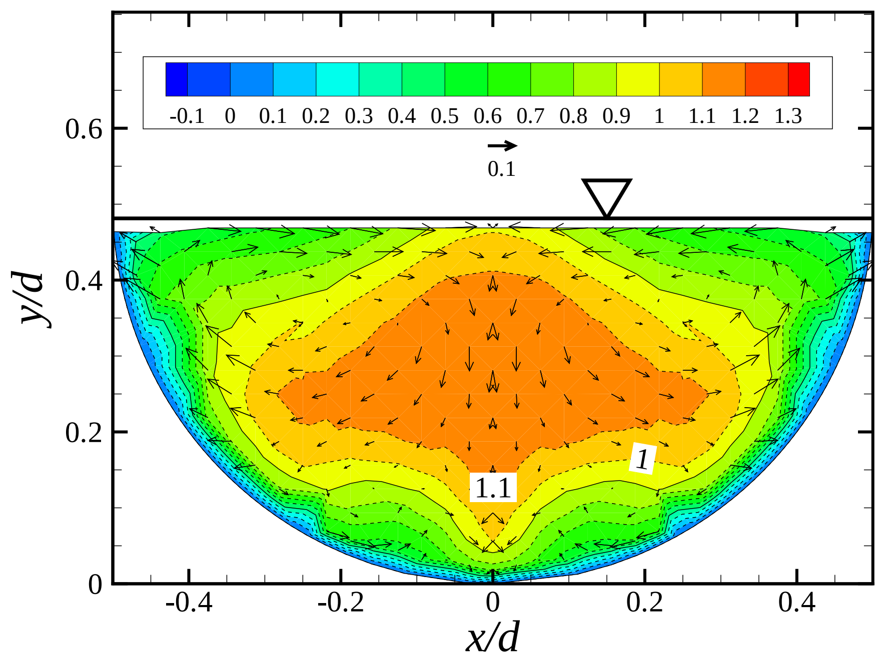

Figure 5-7: Distribution of U/U_{avg} and secondary velocity vectors for the 45° wingwall inlet treatment at a) 0.25D b) 0.5D c) 1D d) 2D

5.3.3 Projecting End

The velocity isovel plot of the 0.25 diameter cross section (Fig. 5-8a), shows that the projecting end inlet causes significant flow separation resulting in a large recirculation zone. A significant portion of the recirculation zone contains negative and stagnant streamwise velocities. The maximum velocity within the cross section is located within triangular jets adjacent to the boundary of the central jet and recirculation zone. The magnitude of the maximum velocity is greater than the other inlet treatments at $1.3U_{avg}$. The velocity gradient between the recirculation zone and central jet is very high. Secondary velocity vectors show contracting flow at the edge of the central jet as well as large vertical and spanwise velocities within the recirculation zone.

At 0.5 diameters downstream of the inlet (Fig. 5-8b), a significant portion of the flow field remains with a streamwise velocity greater than $1.3U_{avg}$. Regions of negative velocity remain within the recirculation zone. The magnitude of secondary velocity vectors have diminished and are negligible near the center of the flow field.

Velocity plots at one diameter (Fig. 5-8c), show that the central jet persists with velocities greater than $1.2U_{avg}$. The velocity gradient between the high and low velocity zones has diminished as the flow begins to reattach to the boundary. Secondary velocity vectors show the expansion of flow near the base of the central jet.

At two diameters downstream of the inlet (Fig. 5-8d), isovel plots show that the flow has reattached to the boundary. A significant portion of the flow field has streamwise velocities less than the average. The maximum velocity region has become depressed below the surface and maintains velocities greater than $1.2U_{avg}$. As with other inlets at two diameters, secondary velocity vectors show weak spiraling secondary circulations.

a)

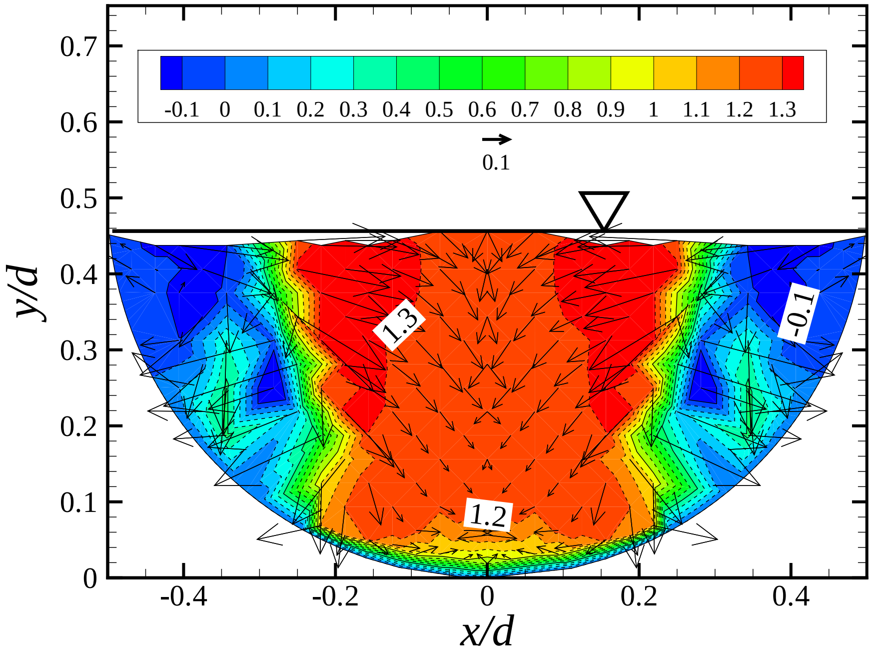
-0.1 0 0.1 0.2 0.3 0.4 0.5 0.6 0.7 0.8 0.9 1 1.1 1.2 1.3
0.1
1.3
-0.1
1.2
y/d
x/d

b)

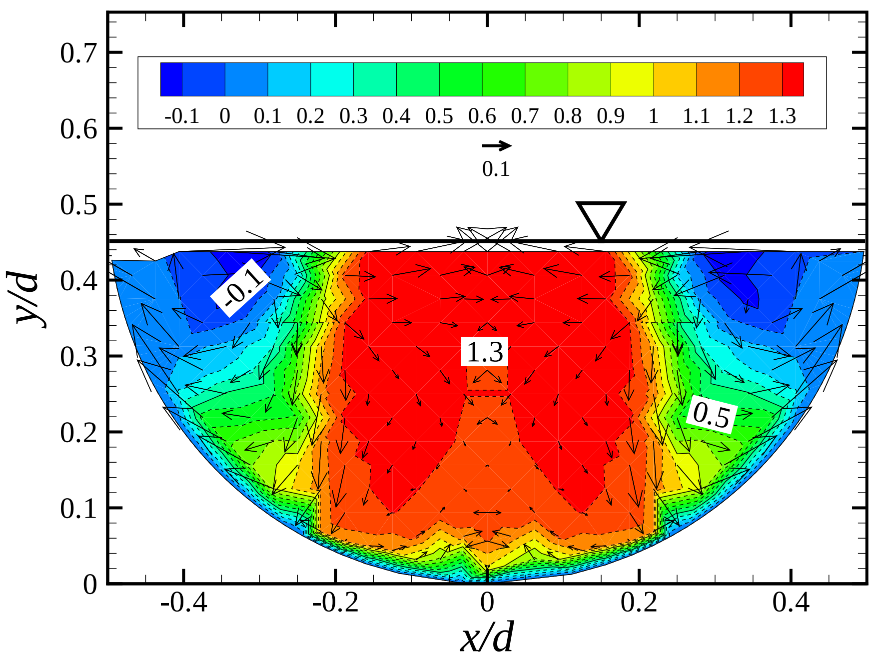
-0.1 0 0.1 0.2 0.3 0.4 0.5 0.6 0.7 0.8 0.9 1 1.1 1.2 1.3
0.1
-0.1
1.3
0.5
y/d
x/d

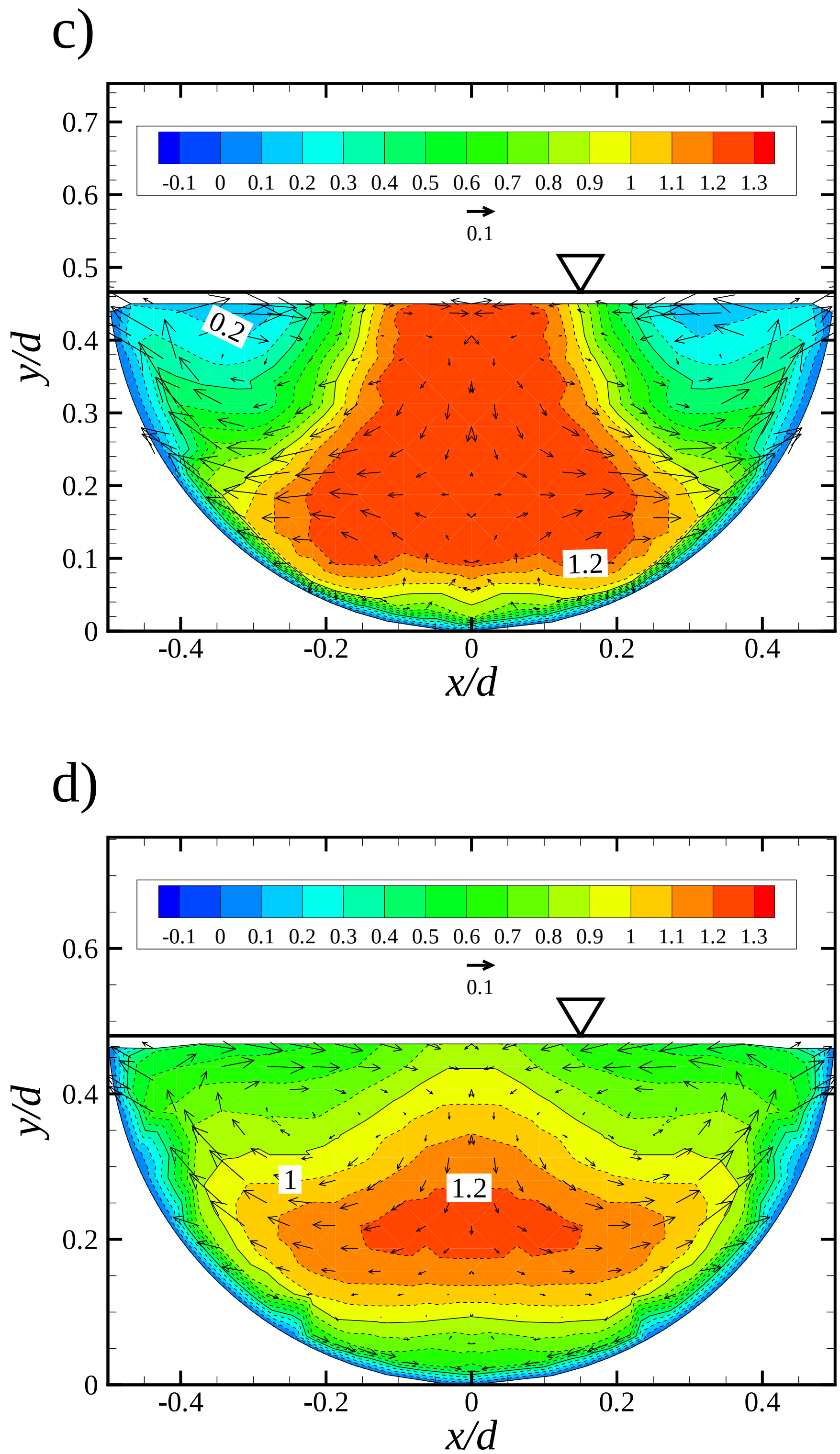

Figure 5-8: Distribution of U/U_{avg} and secondary velocity vectors for the projecting end inlet treatment at a) 0.25D b) 0.5D c) 1D d) 2D

5.3.4 Projecting End Embedded

It should be noted that the increased tailwater depth associated with the embedded test condition results in deeper flow depths than the non embedded configuration and subsequently lower average velocities at each cross section.

The flow structure at 0.25 diameters downstream from the inlet (Fig. 5-9a) is similar to the non embedded configuration however the size of the low velocity recirculation zone has increased and the amount of area with negative streamwise velocities is significantly greater. Within the central jet, the normalized maximum velocity is lower than the non embedded condition at $1.2U_{avg}$. Secondary velocity vectors show plunging and contracting flow within the central jet and significant spanwise velocities within the recirculation zone.

At 0.5, 1 and 2 diameters (Fig. 5-9b-d), the flow structure is similar to the non-embedded configuration, however the maximum velocities are slightly lower as a result of the increased tailwater condition.

a)

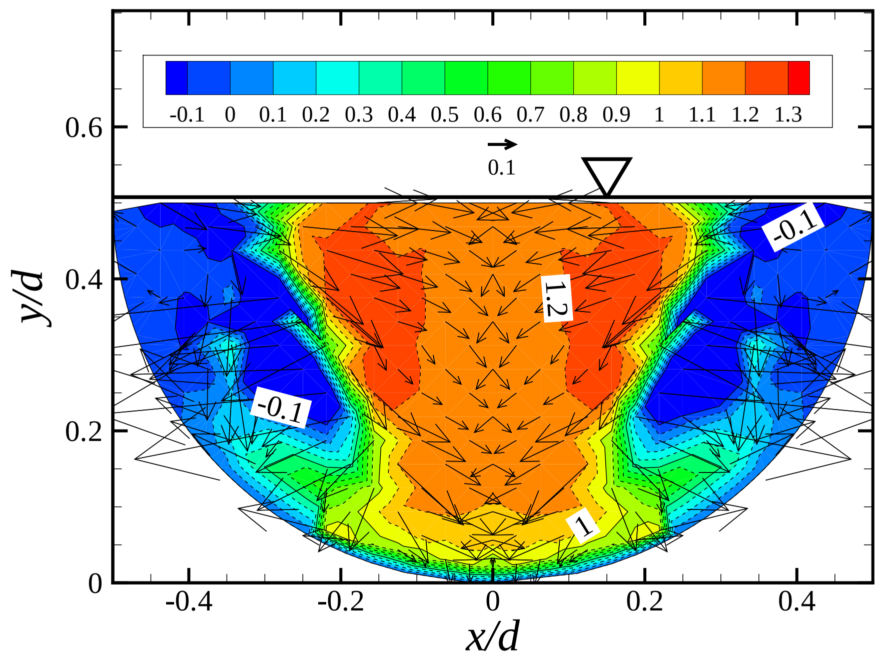
-0.1
0
0.1
0.2
0.3
0.4
0.5
0.6
0.7
0.8
0.9
1
1.1
1.2
1.3
0.1
-0.1
1.2
-0.1
1
y/d
x/d
0.6
0.4
0.2
0
-0.4
-0.2
0
0.2
0.4

b)

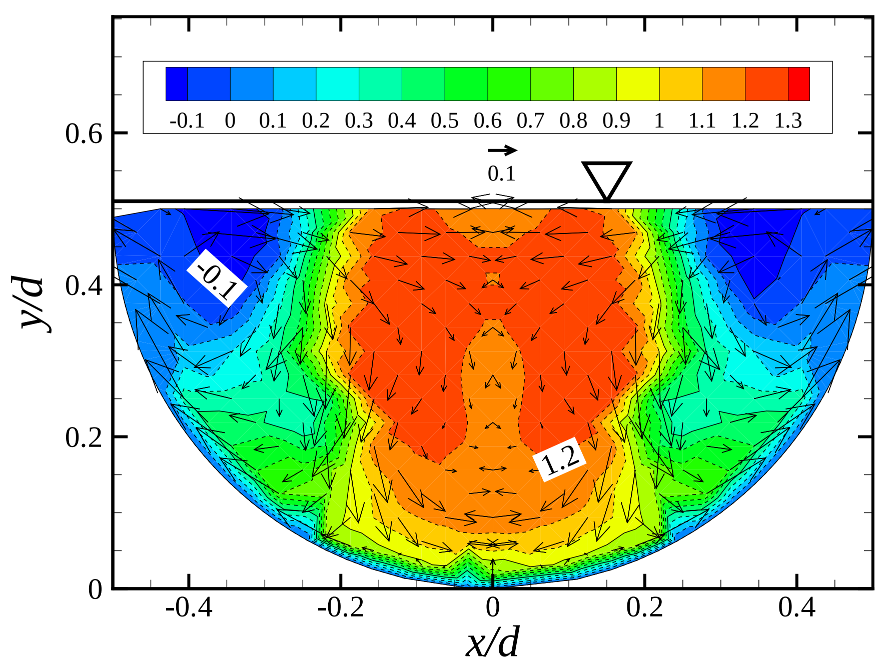
-0.1
0
0.1
0.2
0.3
0.4
0.5
0.6
0.7
0.8
0.9
1
1.1
1.2
1.3
0.1
-0.1
1.2
y/d
x/d
0.6
0.4
0.2
0
-0.4
-0.2
0
0.2
0.4

c)

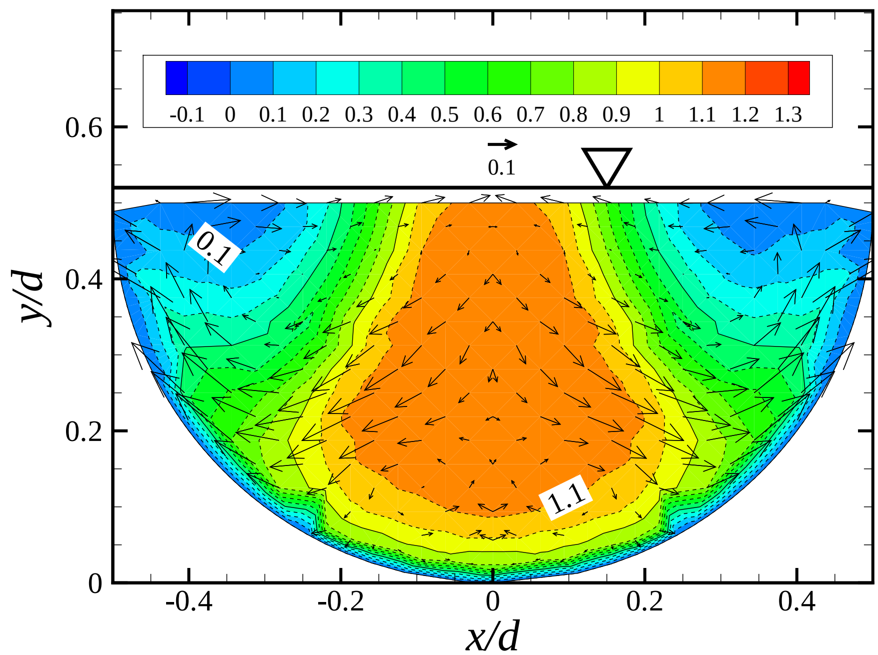

d)

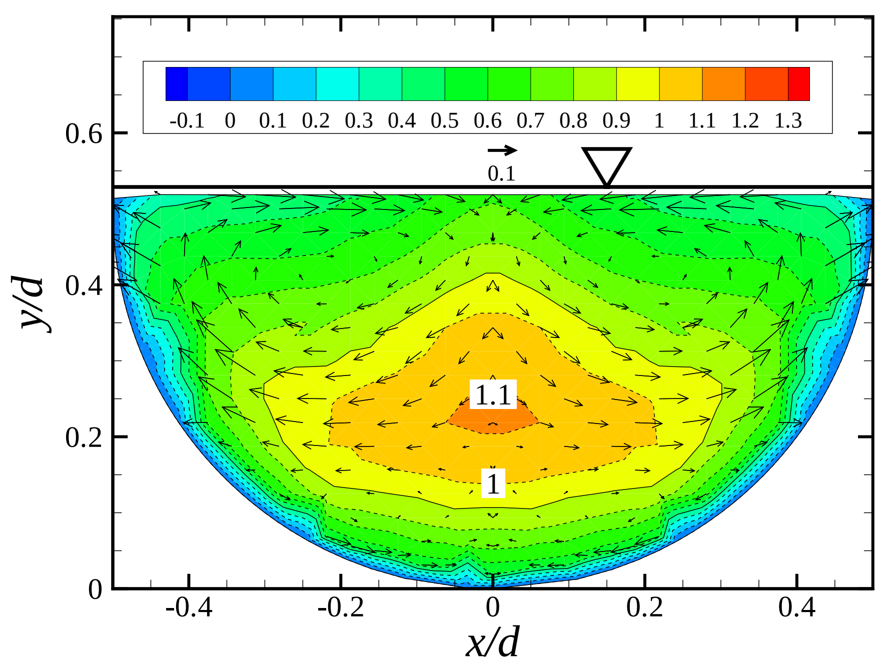

Figure 5-9 Distribution of U/U_{avg} and secondary velocity vectors for the projecting end embedded inlet treatment at a) 0.25D b) 0.5D c) 1D d) 2D

5.3.5 Projecting End Backfilled

Under the backfilled test condition, the velocity distributions along the bed are 'flattened out' presenting a thinner development layer along the bed. The thinner development layer is likely the combined result of having a continuous bed material between the headwater box and culvert as well as the granular material being hydraulically smoother than the annular corrugations of the culvert. This observation is most pronounced at the 0.25 and 0.5 diameter cross sections.

At 0.25 diameters (Fig. 5-10a), the flow field consists of a large low velocity recirculation zone with a significant region of negative streamwise velocities. The central jet again contains triangular lobes of maximum velocity adjacent to the low velocity zone. The 0.5 diameter cross section (Fig. 5-10b), contains significantly less area with velocities above $1.3U_{avg}$. At 1.0 and 2.0 diameters downstream from the inlet (Fig. 5-10c-d), the flow structure is similar to the non-backfilled configuration. The plots agree with the findings of Magura (2007) who used a similar inlet configuration in his study.

a)

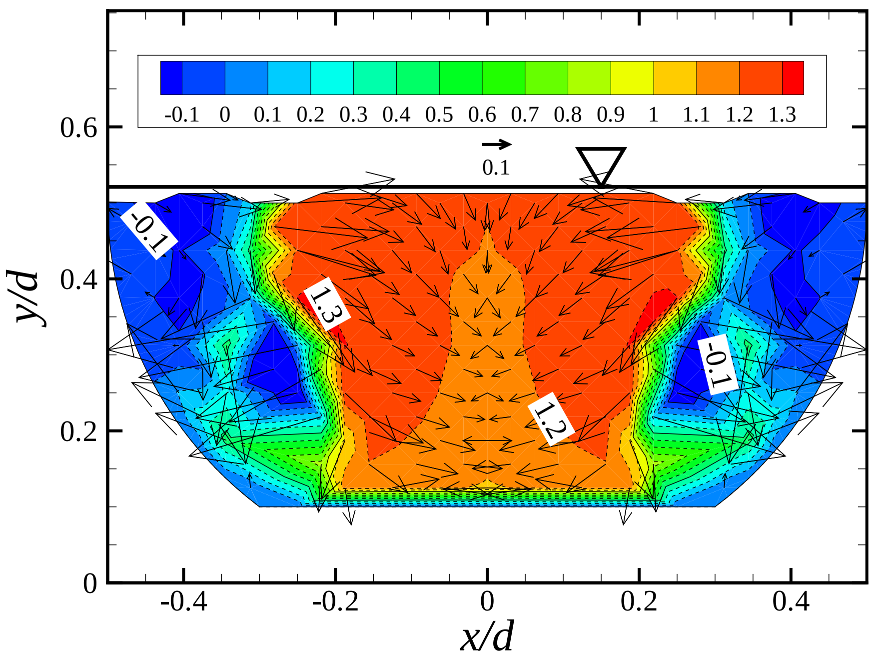
-0.1
0
0.1
0.2
0.3
0.4
0.5
0.6
0.7
0.8
0.9
1
1.1
1.2
1.3
0.1
-0.1
1.3
-0.1
1.2
y/d
x/d
0.6
0.4
0.2
0
-0.4
-0.2
0
0.2
0.4

b)

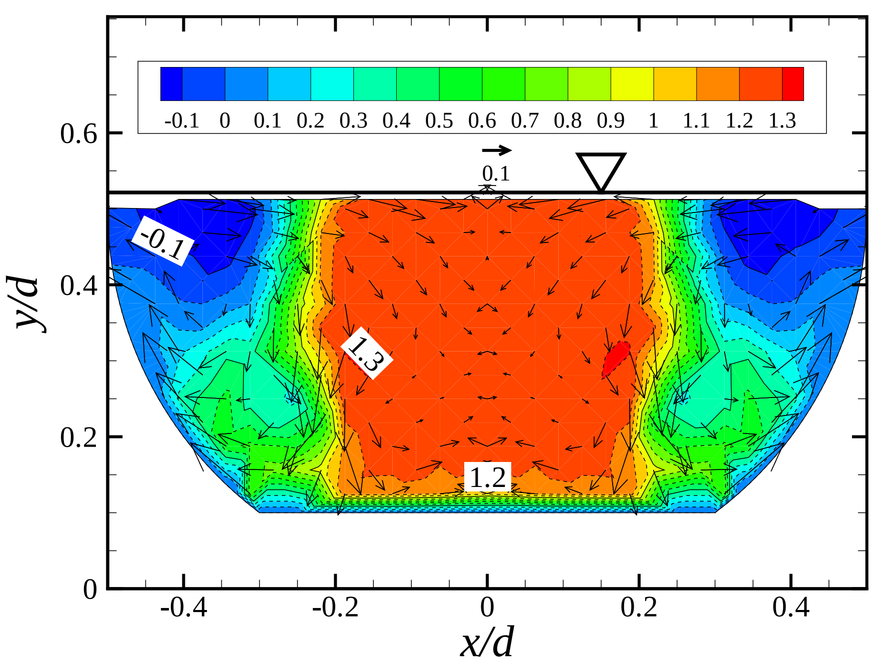
-0.1
0
0.1
0.2
0.3
0.4
0.5
0.6
0.7
0.8
0.9
1
1.1
1.2
1.3
0.1
-0.1
1.3
1.2
y/d
x/d
0.6
0.4
0.2
0
-0.4
-0.2
0
0.2
0.4

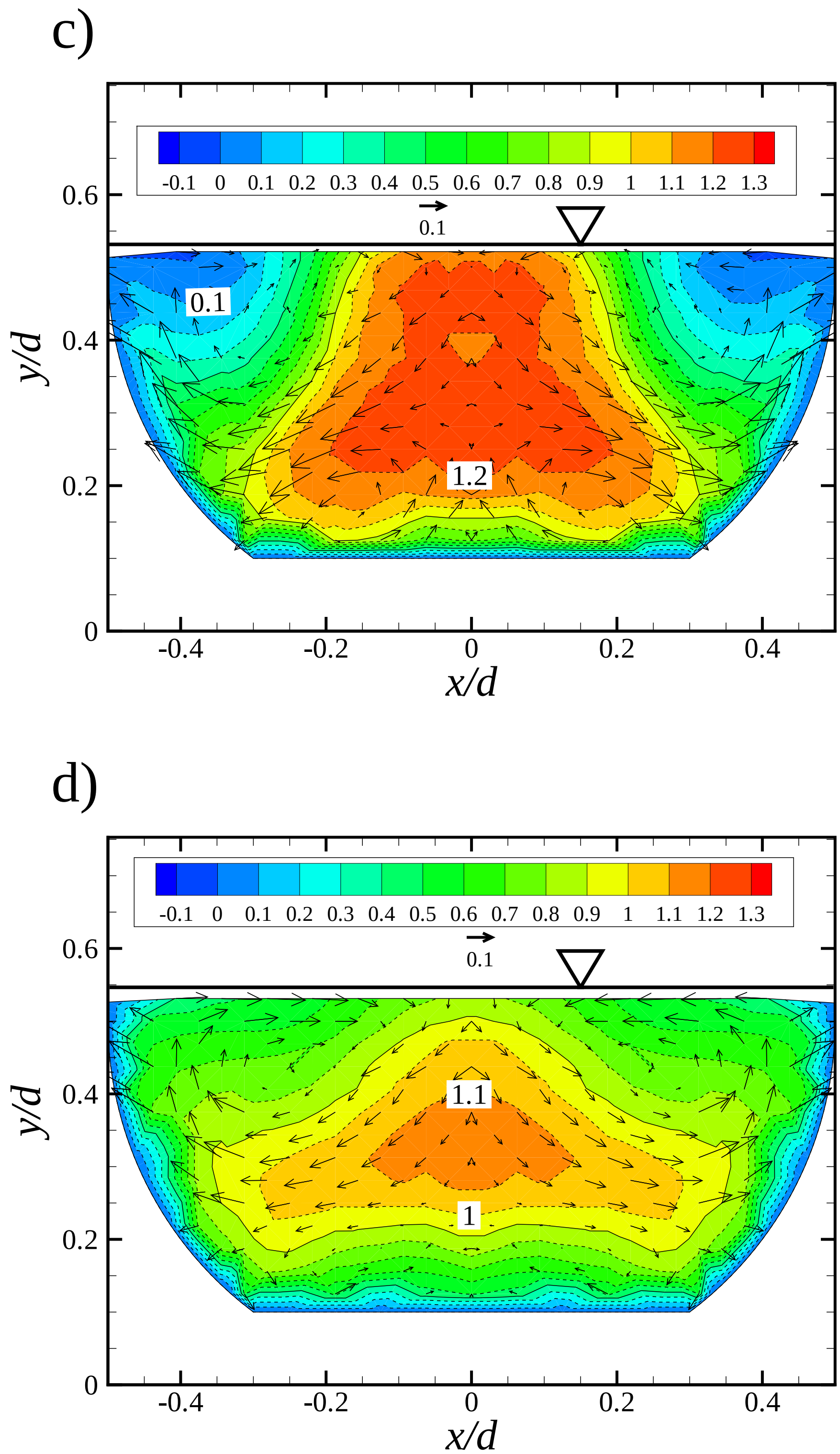

Figure 5-10: Distribution of U/U_{avg} and secondary velocity vectors for the projecting end backfilled inlet treatment at a) 0.25D b) 0.5D c) 1D d) 2D

5.3.6 Percent Area Analysis

In examining the velocity plots, it is evident that with each inlet treatment and at each cross section location a significant amount of the flow field has streamwise velocities less than U_{avg}. In an effort to quantify the extent of low velocity area available as a potential fish passage corridor, the percent area with velocities less than U_{avg} for each inlet configuration at each cross section location were calculated and are plotted in Figure 5-11. It is worth noting that as outlined in Section 4.1 the tailwater level for the embedded and backfilled inlet configurations was raised by the depth of embedment resulting in a slight backwater effect and an M1 profile for these conditions. These differing conditions must therefore be considered when comparing those results to the non-embedded/backfilled configurations.

It was found that for each inlet treatment, the percent area less than U_{avg} increases with distance from the inlet. At each cross section location, the various projecting end inlet configurations possess greater low velocity area than the vertical headwall or 45° wing-wall inlets; which apart from the 0.25 diameter locations are nearly identical. Overall, the projecting end embedded configuration presents the greatest percent area with streamwise velocities less than U_{avg} at each cross section location.

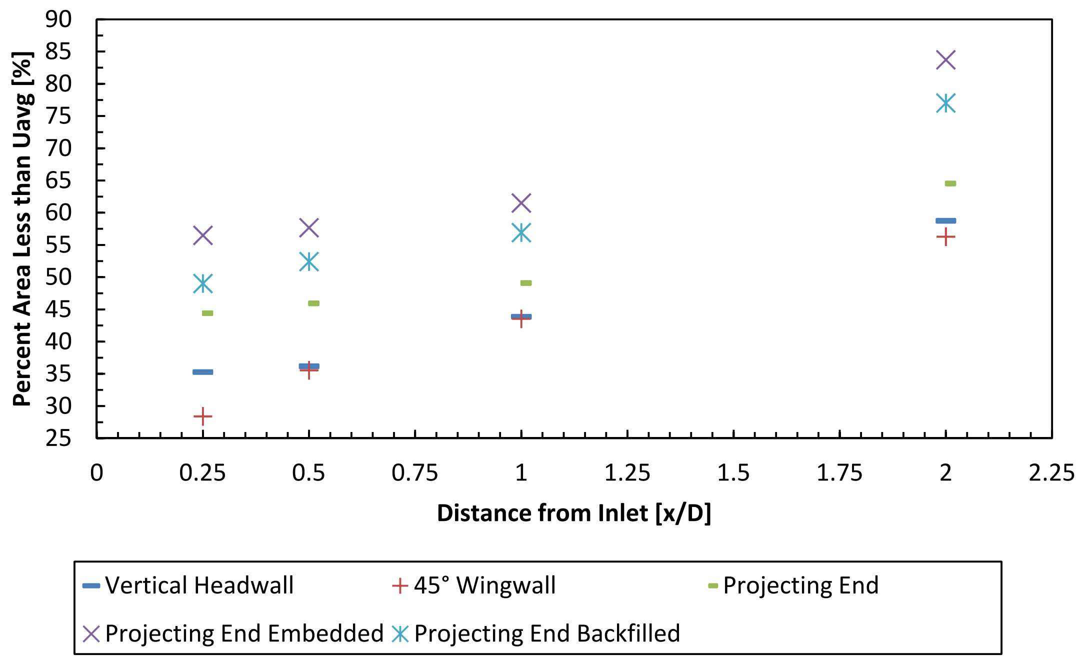

Figure 5-11: Percent Area Less than U_{avg}

5.4 Turbulence

As outlined in Section 2.2.2, the current understanding of how turbulence effects fish passage is not as well developed as it is for velocities. To the author's knowledge, there are few guidelines or regulations stating a limit to the maximum allowable turbulence levels for fish passage in culverts or similar structures. Despite this lack of a clear threshold, it is intuitive that there must be some limit to the level of turbulence a fish would be able to cope with and that the magnitude and or nature of turbulence within a flow must have some effect on a fish's ability to move within it. It is also apparent that the complex flow structures within the inlet region would present some of the greatest levels of turbulence experienced by a fish when ascending a culvert crossing. Gaining an understanding of the turbulent flow conditions within the inlet region of culverts will therefore help designers and regulators compare the relative impact of various inlet treatments.

Towards this end, Figures 5-12 through 5-16, present plots of the normalized turbulent kinetic energy as measured at each of the cross section locations for each of the five inlet configurations. Turbulent kinetic energy was analysed as it encompasses all three dimensions of the flow field and therefore represents the magnitude of turbulence that would be experienced by a fish within those flows. The following paragraphs discuss the distribution of turbulent kinetic energy within the inlet region and provide a comparison between the nature of turbulence levels and structure within the various inlet configurations. Calculated values of k were normalized by the squared average streamwise velocity (U_{avg}^2) within the fully developed region of the culvert. As with the velocity plots, the use of a common normalizing parameter allows for the comparison of figures between cross section locations and inlet configurations. One should note that as the range of observed k varied by orders of magnitude between cross section locations and inlet configurations, the legend associated with each plot is unique and the isovel colours cannot be compared across plots.

5.4.1 Vertical Headwall

The plot of k at 0.25 diameters downstream of the inlet (Fig. 5-12a) shows that elevated levels of k are localized within lobes near the culvert boundary. These lobes correspond to regions of high streamwise velocity gradient found between the high velocity central jet and the low velocity recirculation zone. The maximum values of k also correspond to areas with high spanwise and vertical velocities. The magnitude of maximum normalized *k* found near the center of the lobes is around 1.7. In comparison to the elevated *k* within these concentrated lobes, *k* levels throughout the remainder of the cross section are negligible.

At 0.5 diameters downstream of the inlet (Fig. 5-12b), the plot indicates that elevated *k* levels remain concentrated within the regions associated with the boundary between high and low velocity. The lobes of elevated *k* are no longer as concentrated as at 0.25 diameters corresponding to the diminished velocity gradient. The magnitude of the highest levels of normalized *k* at 0.5 diameters is near 0.13, diminished by an order of magnitude from the maximum found at 0.25 diameters.

At 1.0 diameter downstream of the inlet (Fig. 5-12c), elevated levels of *k* are found along the boundary of the culvert corresponding to areas with a normalized streamwise velocity at or below 1. The maximum value of normalized *k* is approximately 0.09 and is located in a concentrated zone near the upper corners of the cross section. The values of *k* within the central high velocity region remain negligible in comparison to the remainder of the cross section.

By 2.0 diameters downstream of the culvert inlet (Fig. 5-12d), the upper range of *k* has decreased to approximately 0.04. At this location there is no longer a sharp boundary between areas of elevated and low *k*. Higher levels of *k* are located along the water surface and culvert boundary, low levels of *k* are found at the center of the flow field.

a)

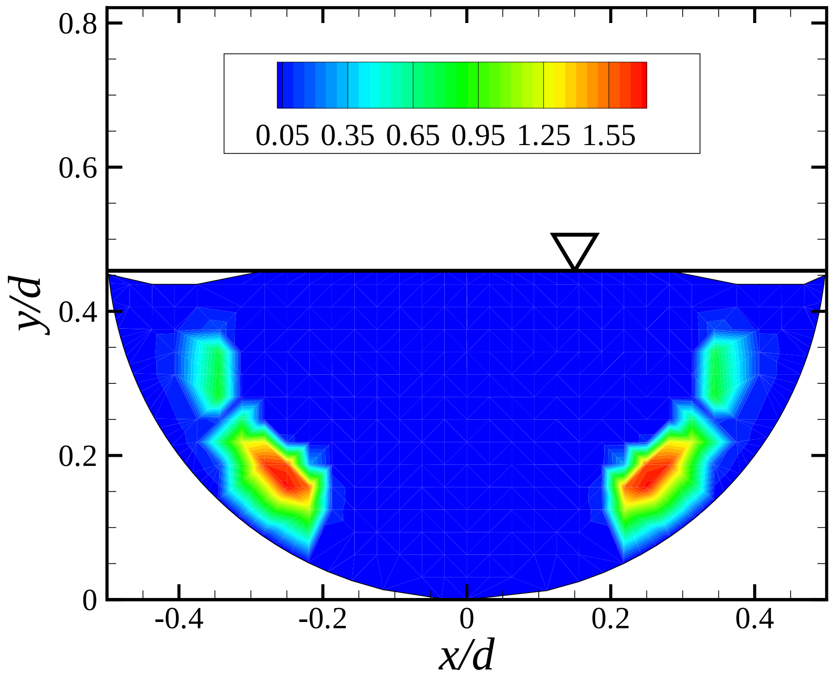
0.05 0.35 0.65 0.95 1.25 1.55
y/d
x/d
0.8
0.6
0.4
0.2
0
-0.4
-0.2
0
0.2
0.4

b)

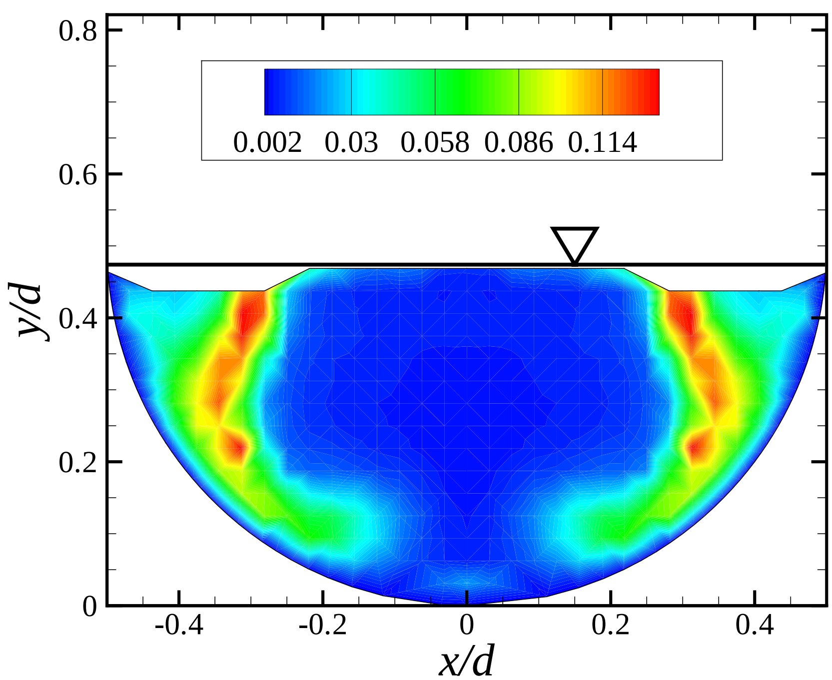
0.002 0.03 0.058 0.086 0.114
y/d
x/d
0.8
0.6
0.4
0.2
0
-0.4
-0.2
0
0.2
0.4

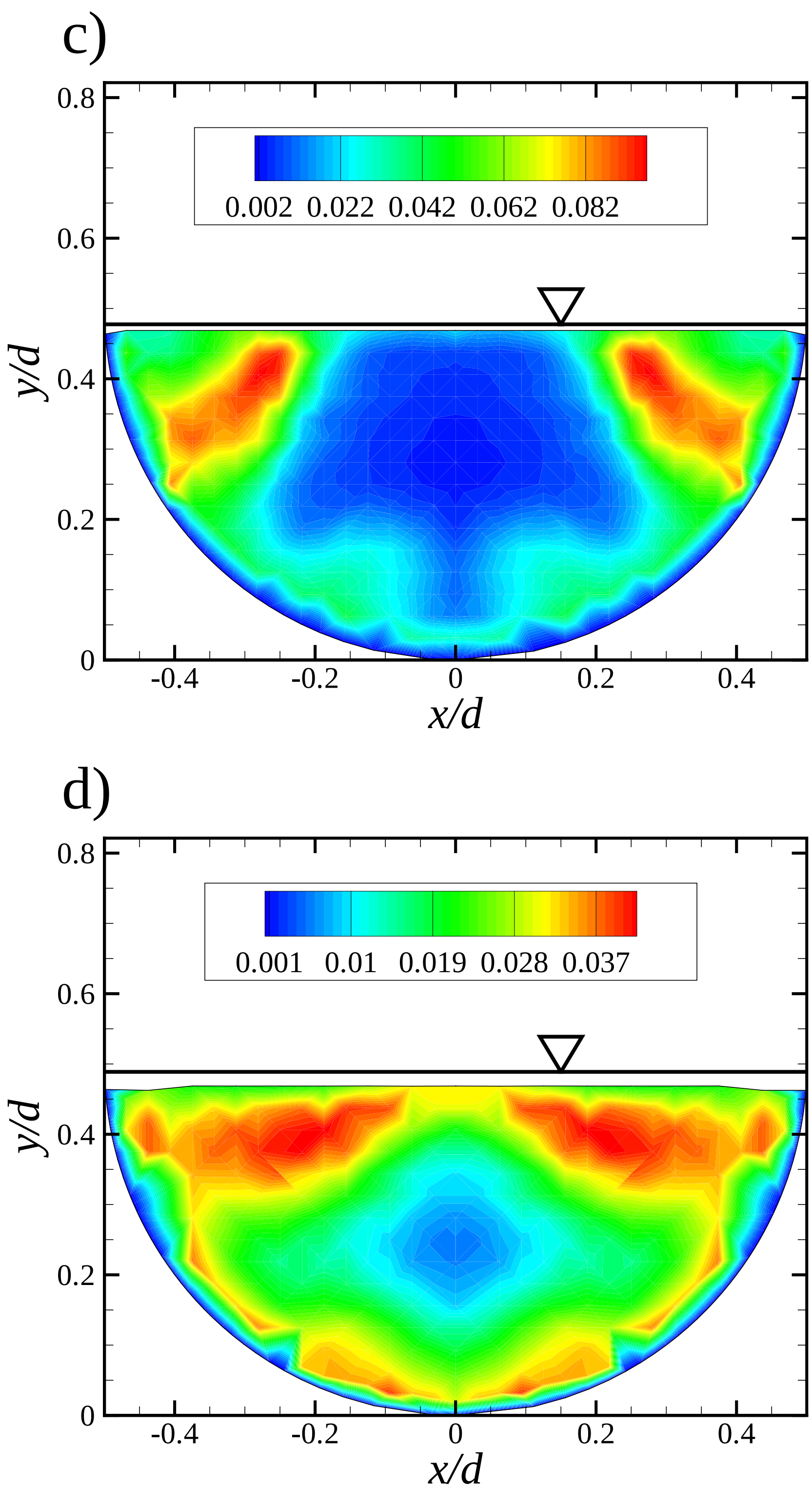

Figure 5-12: Distribution of k/U_{avg}^2 for the vertical headwall inlet treatment at a) 0.25D b) 0.5D c) 1D d) 2D

5.4.2 45° Wingwall

Plots of normalized *k* at 0.25 diameters downstream of the inlet (Fig. 5-13a), indicate that at this location elevated levels of *k* are highly concentrated with an upper range near 0.9 almost half of the upper range observed at this location with the vertical headwall inlet treatment. Levels of *k* throughout the remainder of the cross section are negligible.

At 0.5 diameters downstream of the inlet (Fig. 5-13b), the upper range of *k* has reduced to approximately 0.125, this is similar to the levels observed at this location with the vertical headwall inlet treatment. As with the vertical headwall, inlet regions of elevated *k* correspond to regions with a sharp streamwise velocity gradient.

The upper range of normalized *k* at 1.0 diameters (Fig. 5-13c) has further reduced to around 0.075. The distribution and location of elevated *k* levels has not changed significantly from at 0.5 diameters downstream of the inlet.

At 2.0 diameters downstream of the culvert inlet (Fig. 5-13d), *k* levels and distribution closely resemble those observed with the vertical headwall inlet treatment. The upper range of normalized *k* at this location is approximately 0.035. Levels of *k* within the region of streamwise velocity greater than U_{avg} remain negligible.

a)

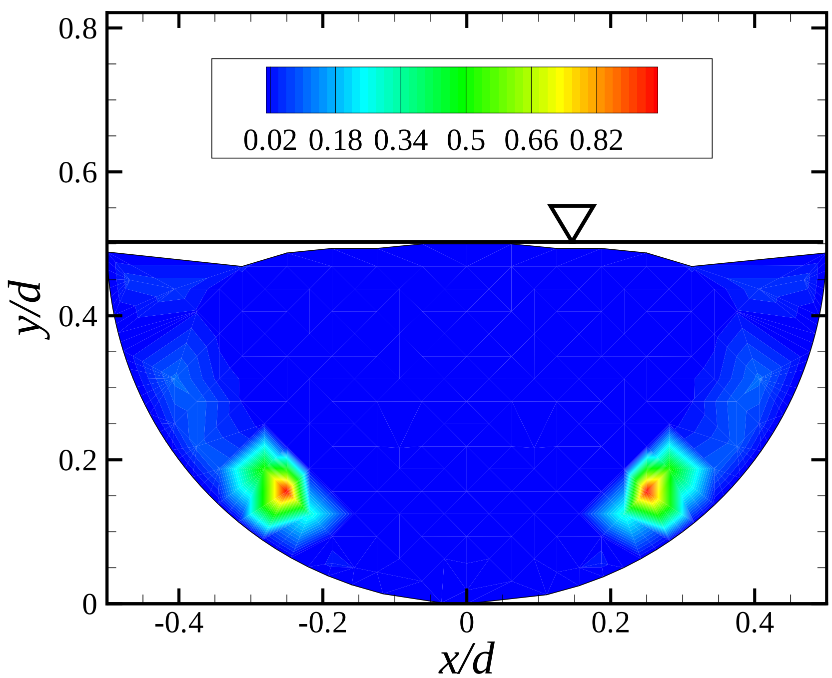

b)

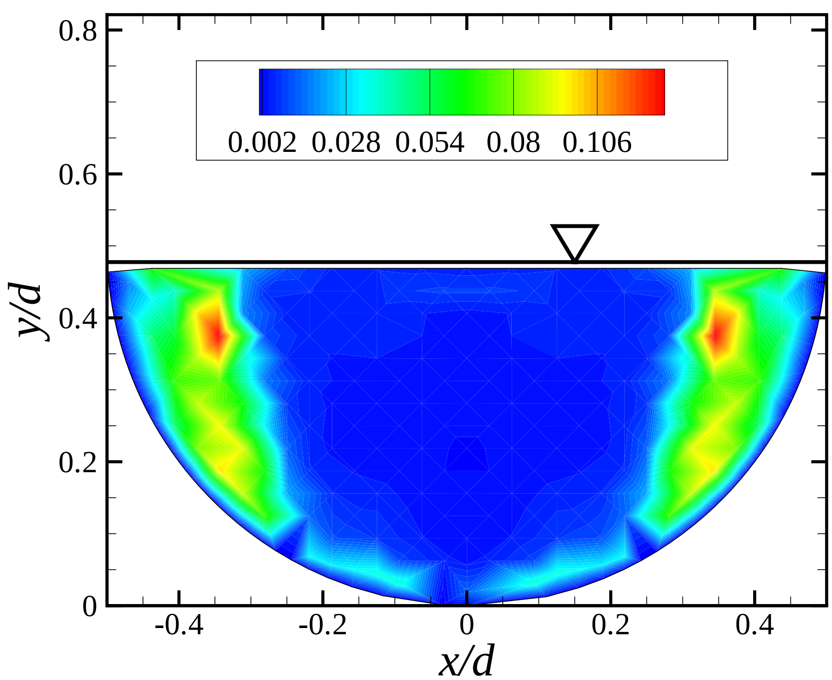

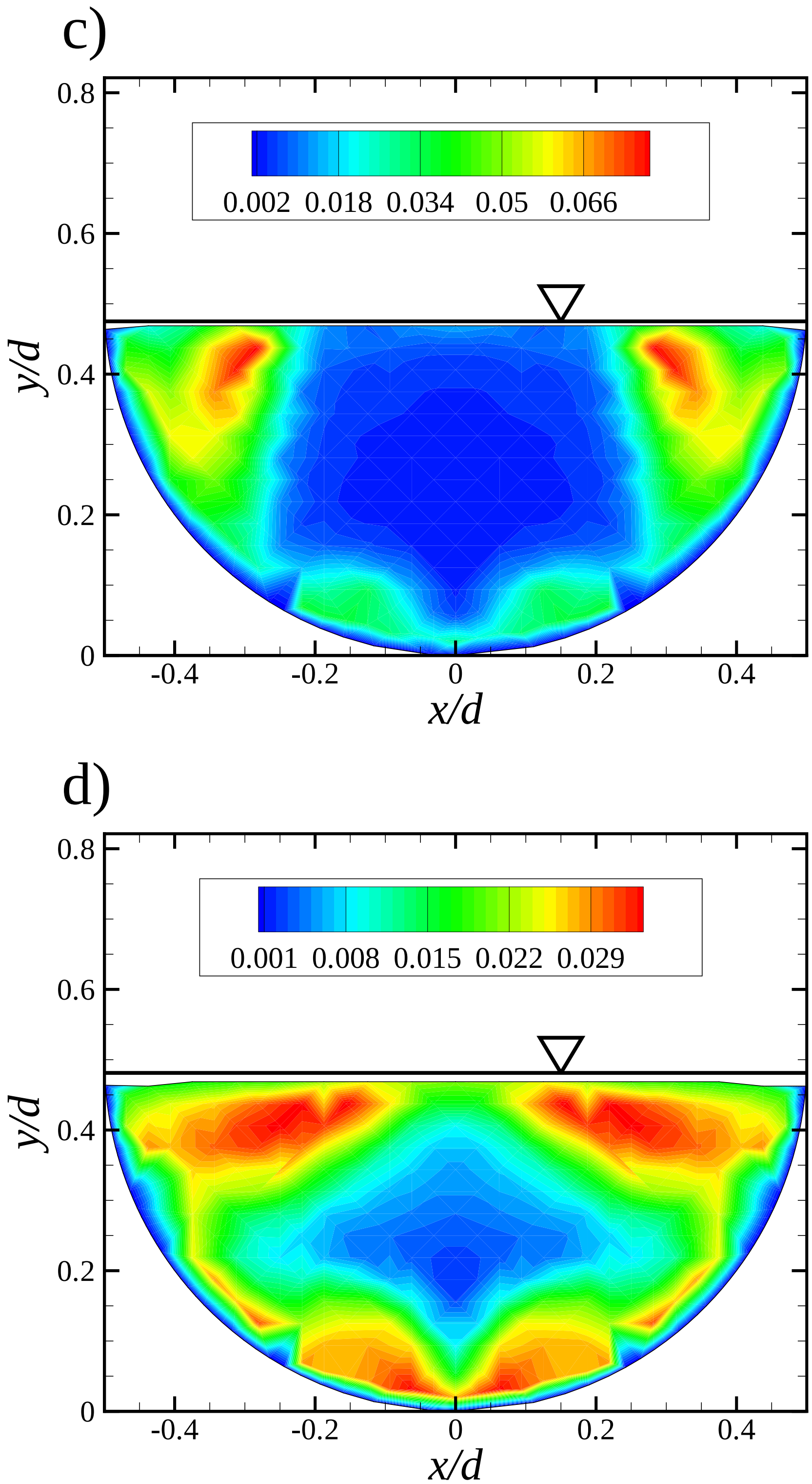

Figure 5-13: Distribution of k/U_{avg}^2 for the 45° wingwall inlet treatment at a) 0.25D b) 0.5D c) 1D d) 2D

5.4.3 Projecting End

The plot of normalized *k* at 0.25 diameters for the projecting end inlet treatment (Fig. 5-14a), demonstrates a similar upper range as the vertical headwall configuration, 1.6 and 1.7, respectively. Also, similar to the vertical headwall inlet treatment, elevated levels of *k* are present within lobes associated with areas of high streamwise velocity gradient.

At 0.5 diameters downstream of the inlet, the plot of normalized *k* (Fig. 5-14b) indicates an upper range of around 0.6. This upper range is significantly higher than those observed for with the vertical headwall and 45° Wingwall inlet treatments, 0.13 and 0.125 respectively. The regions of elevated *k* observed at this cross section are highly concentrated and correspond to areas of high streamwise velocity gradient.

As with the 0.5 diameter location, the normalized *k* plot of the 1.0 diameter cross section (Fig. 5-14c) indicates highly concentrated pockets of elevated *k,* an order of magnitude greater than levels observed at this location with the other inlet treatments, approximately 0.45. Apart from the highly concentrated maximum levels, the overall levels and distribution of *k* within the cross section are similar to the other inlet treatments.

The normalized *k* plot associated with the cross section 2.0 diameters downstream of the inlet (Fig. 5-14d), presents a distribution similar to those presented for the other inlet treatments. The upper range of normalized *k* is slightly higher at approximately 0.06.

a)

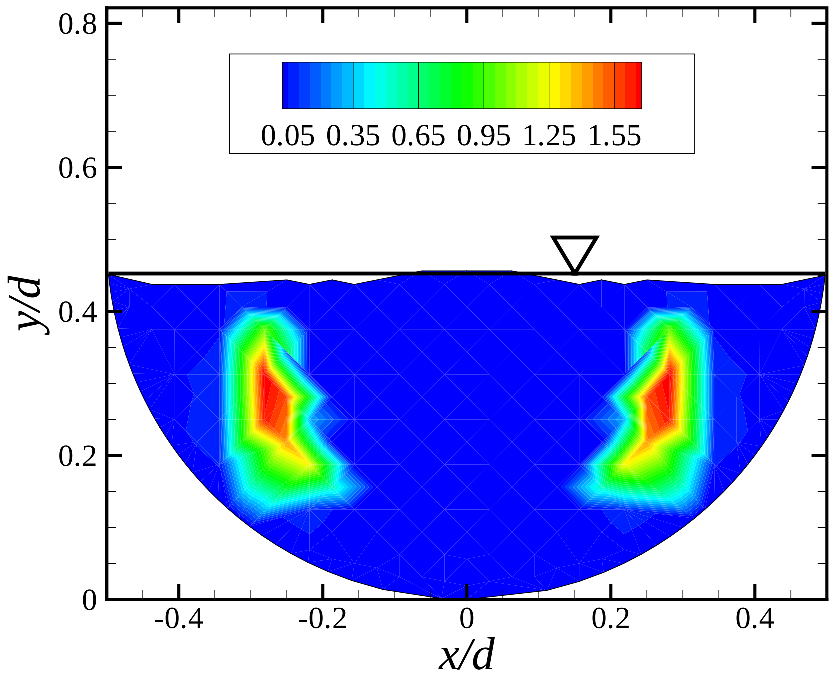
0.05 0.35 0.65 0.95 1.25 1.55
0.8
0.6
0.4
0.2
0
y/d
-0.4
-0.2
0
0.2
0.4
x/d

b)

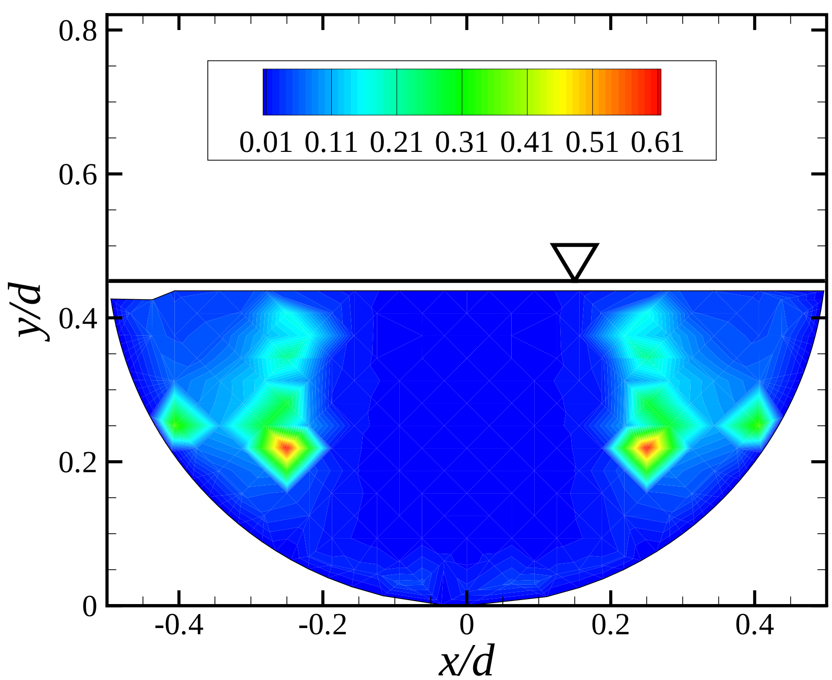
0.01 0.11 0.21 0.31 0.41 0.51 0.61
0.8
0.6
0.4
0.2
0
y/d
-0.4
-0.2
0
0.2
0.4
x/d

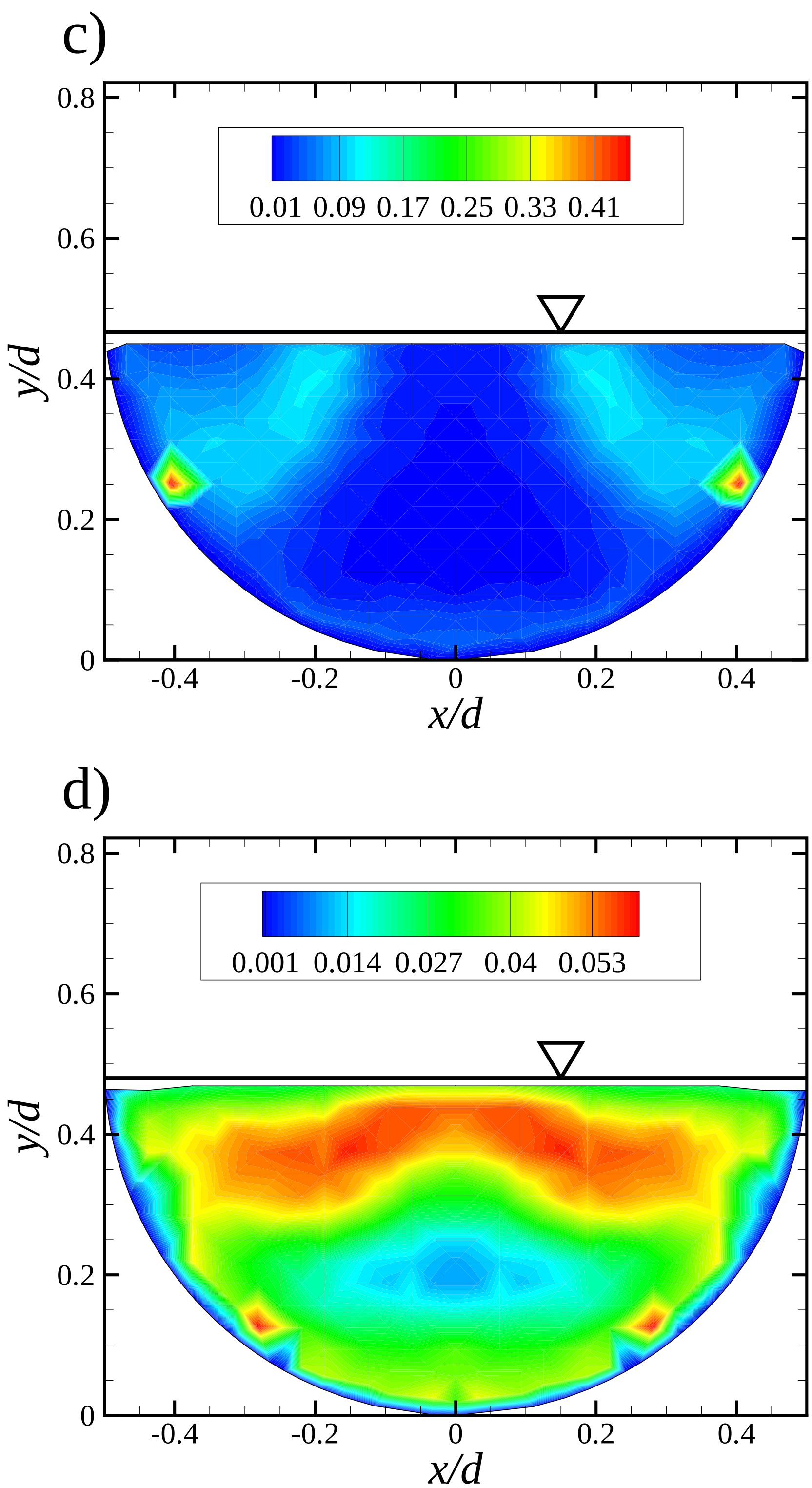

Figure 5-14: Distribution of k/U_{avg}^2 for the projecting end inlet treatment at a) 0.25D b) 0.5D c) 1D d) 2D

5.4.4 Projecting End Embedded

At 0.25 diameters downstream of the inlet (Fig. 5-15a), the projecting end embedded inlet configuration presents a similar distribution of *k* as the non-embedded configuration. The upper range of normalized *k* is approximately 1.7 and as with the other inlet configurations is concentrated within the region of high velocity gradient.

At 0.5 diameters downstream of the inlet (Fig. 5-15b), the upper range of normalized *k* is approximately 1.1, nearly double the level observed with the non-embedded configuration. Apart from the difference in magnitude, the distribution of *k* within the cross section is similar to the non embedded configuration.

At the 1.0 diameter location (Fig. 5-15c), the distribution of normalized *k* for the projecting end embedded configuration resembles those of the vertical headwall and wingwall inlet treatments and does not contain a highly concentrated 'pocket' of elevated *k* as was observed for the non embedded projecting end inlet at this location. The upper range of normalised *k* is approximately 0.11.

At 2.0 diameters downstream of the inlet, the distribution of normalized *k* (Fig. 5-15d) is similar to the distribution of the other inlet treatments with an upper range of approximately 0.055.

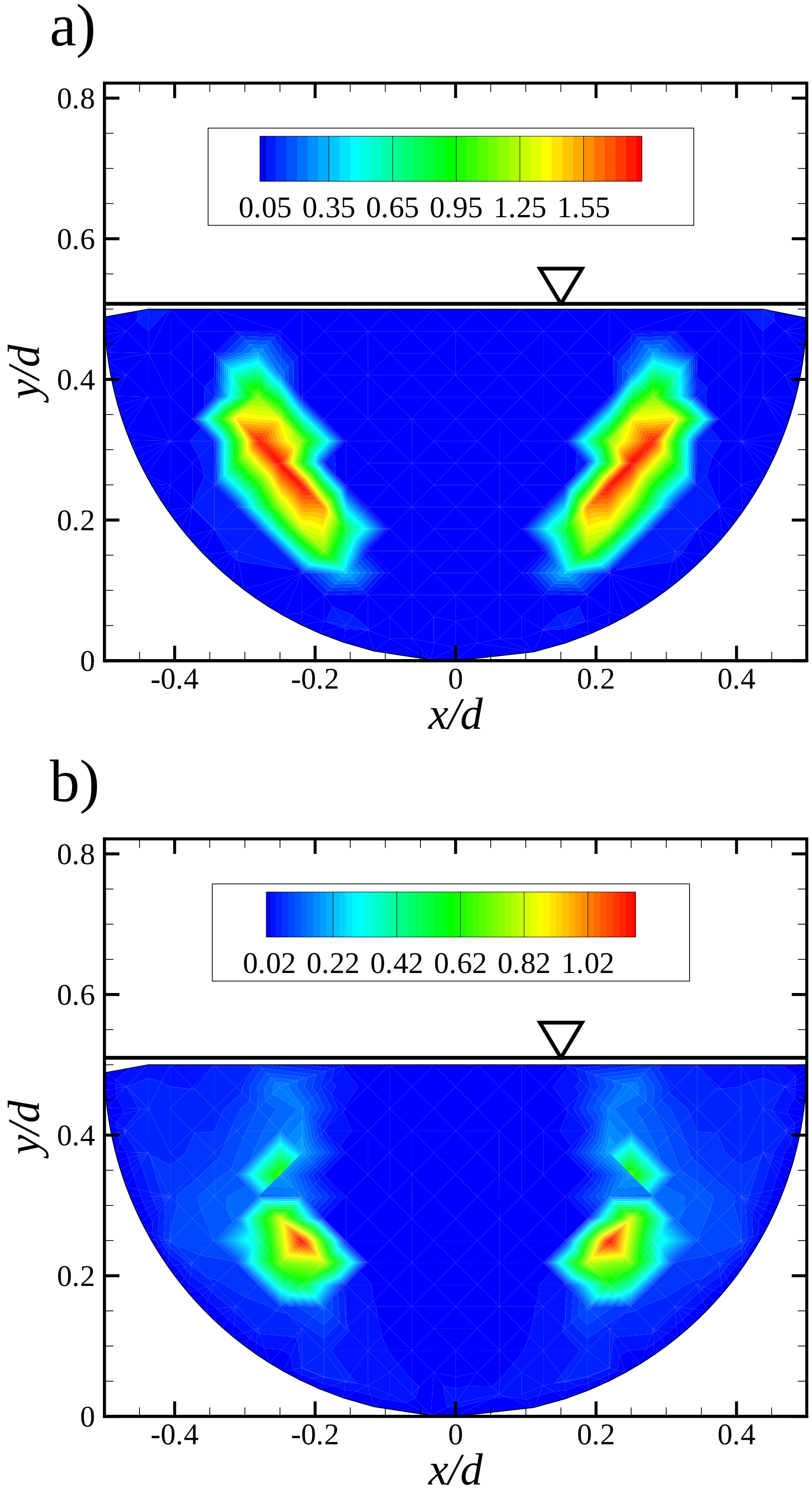
a)
0.05 0.35 0.65 0.95 1.25 1.55
0.8
0.6
0.4
0.2
0
y/d
-0.4 -0.2 0 0.2 0.4
x/d
b)
0.02 0.22 0.42 0.62 0.82 1.02
0.8
0.6
0.4
0.2
0
y/d
-0.4 -0.2 0 0.2 0.4
x/d

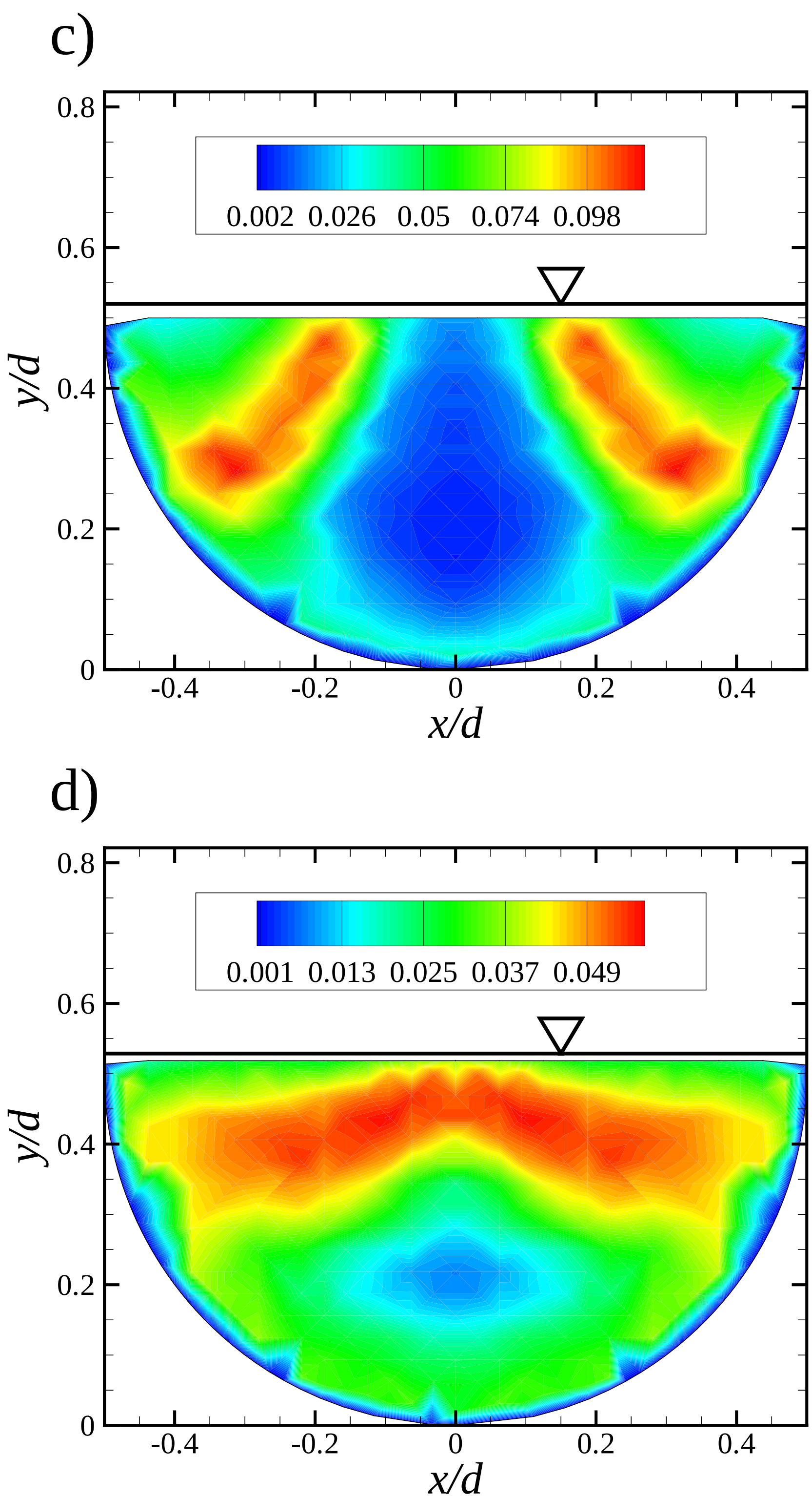

Figure 5-15: Distribution of k/U_{avg}^2 for the projecting end embedded inlet treatment at a) 0.25D b) 0.5D c) 1D d) 2D

5.4.5 Projecting End Backfilled

At 0.25 diameters downstream of the inlet (Fig. 5-16a), the projecting end backfilled inlet configuration presents the highest levels of normalized *k* observed, with a maximum range near 1.8. The position and distribution of the elevated regions of *k* are similar to the other inlet treatments at this location.

The projecting end backfilled configuration again presents the highest recorded values of normalized *k* at the 0.5 diameters location (Fig. 5-16b), at approximately 1.25. The elevated levels of *k* are highly concentrated and *k* throughout the remainder of the cross section is comparatively negligible.

At the 1.0 diameter location (Fig. 5-16c), the distribution of normalized *k* is similar to the non backfilled projecting end configuration with highly localized 'pockets' of elevated *k*. The upper range of normalized *k* within these pockets is approximately 0.35.

By 2.0 diameters downstream of the inlet, the distribution of normalized *k* (Fig. 5-16d) resembles the distribution common to all the other inlet treatments with elevated levels close to the water surface and culvert boundaries, and negligible levels where streamwise velocities are greater than U_{avg}. The upper range of normalized *k* at this location is approximately 0.055.

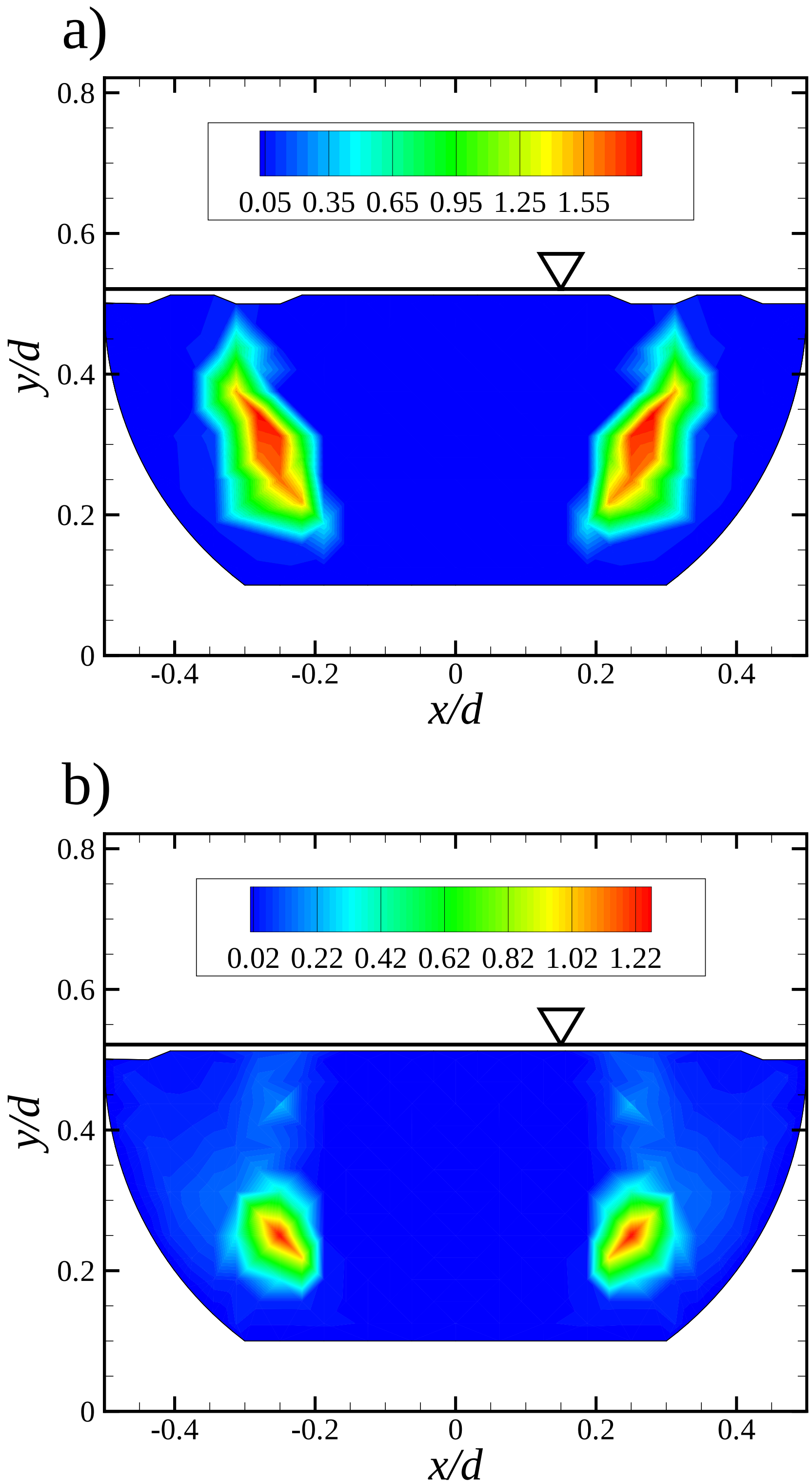
a)
0.05 0.35 0.65 0.95 1.25 1.55
y/d
x/d
0.8
0.6
0.4
0.2
0
-0.4 -0.2 0 0.2 0.4
b)
0.02 0.22 0.42 0.62 0.82 1.02 1.22
y/d
x/d
0.8
0.6
0.4
0.2
0
-0.4 -0.2 0 0.2 0.4

c)

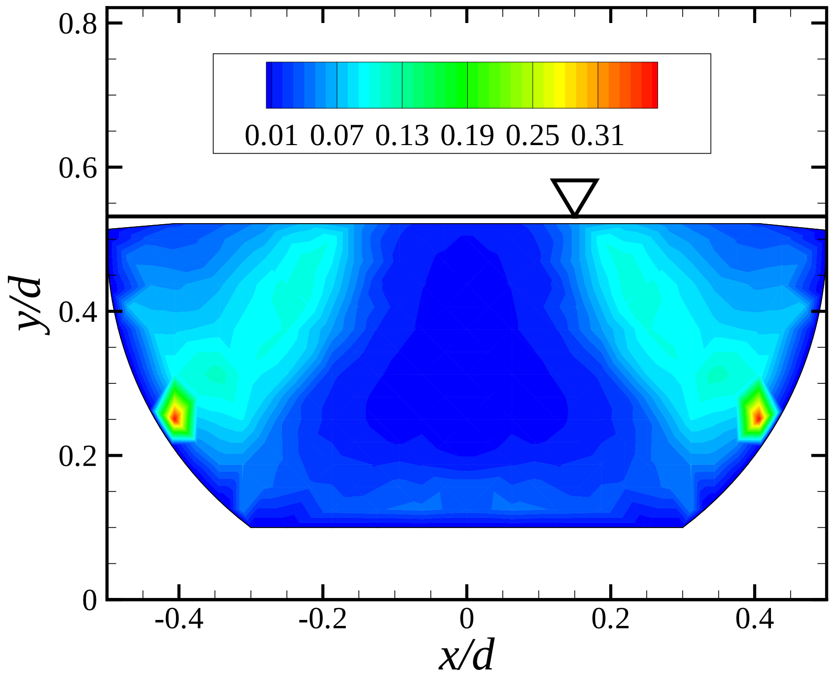

d)

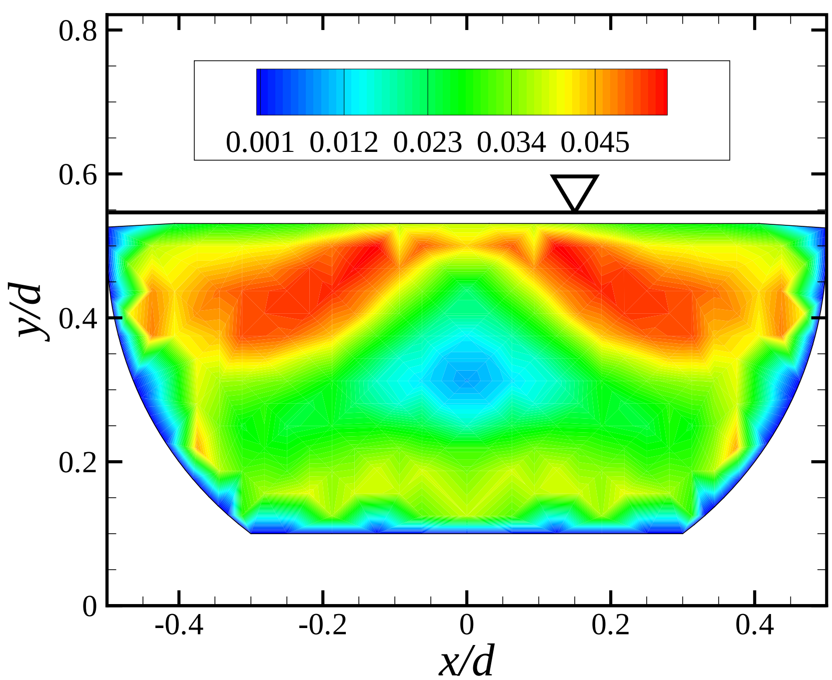

Figure 5-16: Distribution of k/U_{avg}^2 for the projecting end backfilled inlet treatment at a) 0.25D b) 0.5D c) 1D d) 2D

Chapter 6

Conclusions and Recommendations

6.1 Conclusions

The velocity and turbulence field of each inlet configuration examined was characterized by a central jet of high velocity flow surrounded by a low velocity recirculation zone. Turbulence levels were elevated within the low velocity recirculation zone corresponding to locations with significant vertical and spanwise velocities. The magnitude and size of the central jet and low velocity zones varied with each inlet treatment.

Based on percent area analysis, the various projecting end inlet configurations presented the largest area with streamwise velocities less than U_{avg}. Therefore these inlet treatments may present an advantage for fish passage as fish may be able to make use of the low velocity recirculation zones prior to challenging the high velocities just at the lip of the culvert.

However the usefulness of the low velocity recirculation zone as a fish passage corridor may be limited due to the presence of significant vertical and spanwise velocities and corresponding elevated turbulence levels. A fish making use of the low velocity zone would also be required to overcome the virtual mass force, resulting from the acceleration of the fish as it exits the culvert, as well as the accelerating water as it enters the culvert. As this path would likely require the fish to make a burst-type maneuver, its ability to do so would require it to have sufficient capacity remaining in its white muscle energy reserves; this would be dependent on the conditions encountered within the outlet and barrel of the culvert. It is also important to note that the potential benefits associated with the large low velocity recirculation zone need to be weighed against the loss of hydraulic efficiency associated with the increased inlet losses.

The 45° wingwall configuration, presents the hydraulically smoothest transition from the approach zone to the culvert barrel, with lower vertical and spanwise velocities and relatively low levels of turbulence. However, the wingwall inlet provides little to no low velocity recirculation zone reducing the potential for a fish to hold and rest prior to challenging the inlet. The 45° wingwall configuration would therefore present an attractive option for species unsuited to high levels of turbulence and unable to hold within the complex flow patterns of the low velocity recirculation zone. The selection of a wingwall inlet configuration may also be appropriate for crossings with strong swimming fish, capable of traversing the culvert entirely within their prolonged swimming mode.

The embedded projecting end inlet configuration involved lowering the invert of the culvert 0.1 diameters below the stream bed while maintaining the same tailwater condition. This resulted in a slight backwater effect on the inlet and therefore a lower average velocity at each cross section. The cross sectional velocity and turbulence distributions of the embedded configuration were similar to those of the non embedded projecting end configuration with a slight increase in the size of the low velocity recirculation zone. The lower overall velocities presented by this configuration would be a benefit to the passage of weak swimming fish.

The velocity and turbulence distribution of the backfilled inlet configuration presents a different scenario for fish passage in that the boundary layer along the gravel bed is flattened and is thinner than that of the other inlet configurations. This could be a detriment to the passage of species that prefer to travel along the culvert bed. The material used in this study was selected solely based on bed stability without consideration for enhancing fish passage. The use of a substrate with a greater hydraulic roughness would increase the size of the boundary layer and could improve passage conditions for bottom orientated fish.

The successful design of a stream crossing should consider a balance between the needs of fish to move freely within a watercourse and the requirement to develop safe and cost effective infrastructure. As such, the design of a CSP culvert crossing should be undertaken as an interdisciplinary exercise combining the findings of this and other hydraulic studies with a detailed understanding of the behaviour/capability of the target fish species.

6.2 Recommended Future Work

Based on the review of existing literature and the findings of this study, the following list of future work is provided to help guide the further development of fish passage in relation to the design of culvert crossings:

- Due to the time-consuming nature of the laboratory component of this study only a limited number of inlet configurations and hydraulic parameters were examined. Future studies should examine the effect of alternative culvert shapes, embedment depths, and bed material gradations.
- A field or laboratory study should be conducted to examine the behaviour of fish within culvert crossings with the aim of determining if fish (or which species) make use of the lower flow velocities within the boundary layer and recirculation zones.
- The effects of turbulence on non-salmonid fish species should be examined, with the goal of developing criteria to guide the design of culverts and other structures.
- An interdisciplinary approach to the development of improved culvert design guidelines should be undertaken combining the current understanding of detailed culvert hydraulics with a biological understanding of fish behavior/capability.

Bibliography

Abbs, T., Kells, T. J., & Katopodis, C. (2007). A Model Study of the Hydraulics Related to Fish Passage Through Backwatered Culverts. *Proceedings of the 18th CSCE Hydrotechnical Conference* . Winnipeg.

Behlke, E. C., Kane, L. D., McLean, F. R., & Travis, D. M. (1991). *Fundamentals of culvert design for the passage of weak-swimming fish.* Fairbanks: Alaska DOT & PF.

Bell, M. C. (1986). *Fisheries handbook of engineering requirments and biological criteria.* Portland: U.S. Army Corps of Engineers, Fish Passage Development and Evaluation Program.

Bodhaine, G. L. (1976). *Measurment of peak discharges at culverts by indirect methods.* Washington, D.C.: Goverment Printing Office, U.S. Geological Survey.

Brandt, M. M., Holloway, J. P., Myrick, A. C., & Kondratieff, C. M. (2005). Effects of waterfall dimensions and light intensity on age-0 brook trout jumping performance. *Transactions of the American Fisheries Society* , vol. 134, no2, pp. 496-502 .

Canadian Depardment of Fisheries and Oceans and Manitoba Natural Resources. (1996). *Manitoba stream crossing guidelines for the protection of fish and fish habitat.* Winnipeg.

Chow, V. T. (1959). *Open Channel Hydraulics.* New York: McGraw-Hill.

Day, R. A. (1993). *The hydraulic characteristics of culverts.* Wallingford: University of Hertsfordshire.

Department of Fisheries and Oceans . (1985). *Fisheries Act.* Ottawa: Government of Canada.

Ead, S., Rajaratnam, N., Katopodis, C., & Ade, F. (2000). Turbulent open-channel flow in circular corrugated culverts. *Journal of Hydraulic Engineering* , 126(10), 750-757.

Federal Highway Administartion. (2001). *Hydraulic design of highway culverts.* Virginia: National highway institute.

Federal Highway Administration. (2007). *Design for fidh passage at roadway-stream crossings: Synthesis Report.* Virginia: U.S. Department of Transportation.

French, R. (1985). *Open-channel hydaulics.* Ney York: McGraw-Hill.

Goring, D., & Nikora, V. (2002). Despiking Acoustic Doppler Velocimeter Data. *Journal of Hydraulic Engineering* , Vol. 128, No. 1, pp. 117-126.

Kehler, N. J. (2009). *Hydraulic characteristics of fully developed flow in circular culverts.* Winnipeg: University of Manitoba.

Magura, C. (2007). *Hydraulic characteristics of embedded circular culverts.* Winnipeg: University of Manitoba.

Nezu, I., & Nakagawa, H. (1993). *Turbulence in Open-Channel Flows.* Balkema.

Papanicolaou, A., & Talebbeydokhti, N. (2002). Discussion of “Turbulent open-channel flow in circular corrugated culverts” by S.A. Ead, N. Rajaratnam, C. Katopodis, F. Ade. *Journal of Hydraulic Engineering* , vol 145, 547–548.

Pope, S. B. (2000). *Turbulent Flows.* Cambridge: Cambridge University Press.

Smith, L. D., Brannon, L. E., Shaffi, & Odeh. (2006). Use of average and fluctuating velocity components for estimation of volitional rainbow trout density. *Transactions of the American Fisheries Society* , vol 135:2, 431-441.

SonTec. (2001). *ADVfeild acoustic doppler velocimeter technical documentation.* San Diego: SonTec Systems.

Stuart, T. (1962). *The leaping behaviour of salmon and trout at falls and obstuctions.* Edinburgh : Department of Agriculture and Fisheries Scotland.

Sturm, T. W. (2001). *Open channel hydraulics.* New York: McGraw-Hill.

Tullis, B. P., Anderson, D. S., & Robinson, S. C. (2008). Entrance Loss Coefficients and Inlet Control Head–Discharge Relationships for Buried-Invert Culverts. *Journal of Irrigation and Drainage Engineering* , vol. 134(6), 831-839.

Webb, P. W. (1975). *Hydrodynamics and energetics of fish propulsion.* Ottawa: Department of the Environment, Fisheries and Marine Service.